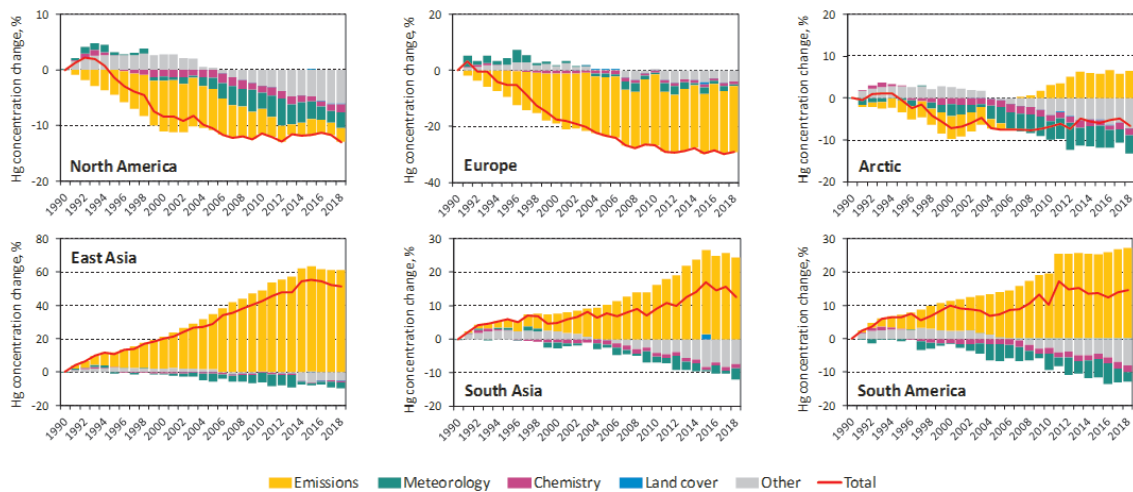


Co-operative activities on Hg and POP pollution assessment within TF HTAP

Progress Report



Technical Report 1/2021

MSC-E Technical Report 1/2021

July 2021

Co-operative activities on Hg and POP pollution assessment within TF HTAP

Progress report

METEOROLOGICAL SYNTHESIZING CENTRE - EAST

Oleg Travnikov, Mikhail Kleimenov and Aleksey Gusev



Meteorological Synthesizing Centre - East

2nd Roshchinsky proezd, 8/5, 115419 Moscow, Russia

Phone.: +7 926 292 00 18, E-mail: msce@msceast.org

www.msceast.org

CONTENTS

1. Introduction	5
2. TF HTAP Workshops on Hg and POP research activities	6
2.1. Workshop on Hg	6
2.2. Workshop on POPs	8
3. Pilot analysis and attribution of long-term Hg and POP pollution trends	10
3.1. Model setup and experiments	10
3.2. Input data	12
3.2.1. Meteorological data	12
3.2.2. Chemical reactants	13
3.2.3. Land cover	15
3.2.4. Emissions	16
3.3. Long-term changes of Hg pollution	20
3.3.1. Observed and modelled temporal trends	22
3.3.2. Trends attribution to regional and extra-regional emissions	23
3.3.3. Trends attribution to environmental factors	24
3.4. Long-term changes of POP pollution	26
3.4.1. Observed and modelled temporal trends	28
3.4.2. Trends attribution to regional and extra-regional emissions	29
3.4.3. Trends attribution to environmental factors	31
4. Concluding remarks	34
References	36

1. Introduction

Mercury (Hg) and POPs are toxic pollutants capable of transport and bioaccumulation in the environment as well as adverse effects on human health and ecosystems. Due to long residence time in the atmosphere and cycling among the environmental media Hg and some POPs can be transported over long distances. Intercontinental transport of these pollutants can significantly contribute to pollution levels, particularly, in regions with low domestic emissions. Therefore, evaluation of present-day Hg and POP pollution, historical trends as well as forecasts of future changes have to take into account emission changes in various continents and the global character of their dispersion.

Mercury and POP pollution is a subject of regulatory activities of many national and international organizations including the UNECE Convention on Long-range Transboundary Air Pollution (Air Convention), the UN Environment Programme, the Minamata Convention on Mercury, the Stockholm Convention on POPs, the Arctic Monitoring and Assessment Programme (AMAP), the HELCOM and OSPAR marine conventions, etc. Efforts aimed at consolidating international activities on Hg and POP pollution assessment were undertaken under the Task Force on Hemispheric Transport of Air Pollution (TF HTAP) of the Air Convention's Cooperative Programme for Monitoring and Evaluation of the Long-range Transmission of Air Pollutants in Europe (EMEP). In particular, results of the cooperative work of the international scientific community on evaluation of Hg and POP pollution on a global scale were included to the TF HTAP Assessment 2010 [*HTAP*, 2010a; *HTAP*, 2010b].

Recently TF HTAP resumed cooperative activities on Hg and POPs research and assessment. In particular, the Task Force jointly with the Meteorological Synthesizing Centre – East of EMEP (MSC-E) hosted two workshops on Hg and POPs, respectively, to identify near-term opportunities and longer-term research needs to improve the scientific basis for assessment of Hg and POP pollution and trends. The workshops examined current efforts throughout the international science community and initiated cooperative work aimed at revealing additional issues or measures that might be addressed to protect the environment and human health. Attribution of long-term pollution trends is considered as one of the perspective directions of the Task Force future activities.

Analysis of long-term pollution trends involving both measurement data and modelling results is widely used for the effectiveness evaluation of the environment protection measures [e.g. *Colette et al.* 2016; *UNEP*, 2017; *AMAP/UNEP*, 2019]. Changes of pollution levels in particular regions are determined by reduction of anthropogenic emissions as a result of mitigation efforts as well as by other factors including changes in meteorological conditions, chemical properties of the atmosphere, surface characteristics etc. Thus, analysis of the factors responsible for pollution changes in the past can provide useful information for developing effective strategies of environmental protection in the future.

The current progress report contains information on discussions and the main outcome of the TF HTAP Workshops on Hg and POPs (Chapter 2). Besides, the results of pilot simulations and the trend attribution analysis performed by MSC-E on a global scale are presented in Chapter 3 to facilitate further discussion and reveal possible issues and uncertainties of the research. Finally, the main conclusions and directions of future research are formulated in Chapter 4.

2. TF HTAP Workshops on Hg and POP research activities

In accordance with the bi-annual work plan of the Convention for 2020-2021 [ECE/EB.AIR/144/Add.2] TF HTAP and MSC-E jointly hosted two exploratory workshops to identify near-term opportunities and longer-term research needs to improve the scientific basis for assessment of pollution and trends of Hg (13 April 2021, online) as well as POPs and Chemicals of Emerging Concern (CEC) (15 April 2021, online) on regional and global scales. The workshops were particularly focused on:

- Reviewing progress made and anticipating assessment needs of the Air Convention, the Minamata Convention, Arctic Monitoring and Assessment Programme, and other international forums;
- Identifying cooperative activities that can be undertaken in the short term (2 years) and longer term (5 years) to improve our understanding and ability to estimate Hg pollution levels, trends and source attribution.

Main topics of discussion and outcomes of the workshops are summarized below.

2.1. Workshop on Hg

The Workshop on Hg was aimed at initiating cooperative research activities to better assess the regional and extra-regional contribution to long term trends of Hg and identify additional issues or measures that might be addressed by the Air Convention to protect the environment and human health. Besides, recognizing that the Hg pollution issue is addressed in other international bodies the future work of TF HTAP will be designed to both build upon the findings of recent efforts in other forums and provide useful information back to the forums to the extent possible.

Attended by 85 international experts, the workshop examined current work and efforts throughout the international science community and under various international organizations addressing Hg pollution problem. During the meeting, participants explored potential synergies with the on-going activities under the Minamata Convention on Mercury (MCM), UN Environment Global Mercury Fate and Transport Partnership (UNEP F&T), Global Observation System for Mercury (GOS4M), the Global Mercury Observation Training Network project (GMOS-Train), Arctic Monitoring and Assessment Programme (AMAP), national Hg pollution assessment programs in China, and identified areas where new cooperative efforts under the Task Force could be most impactful.

At the meeting a discussion of policy-relevant science questions was initiated to govern future cooperative research of Hg regional and global pollution within TF HTAP. A preliminary list includes the following questions:

1. What are the observed and modelled trends in air concentration and deposition of Hg in the UNECE region and other regions of the globe?
2. To what extent are these trends associated with emission changes in the regions or dependent on intercontinental transport of Hg and other environmental factors?

3. What are the relative contributions and their changes of anthropogenic, geogenic, and legacy emission sources to Hg air concentration and deposition in various regions?
4. How may Hg air concentration and deposition levels and the contribution of various sources change in future due to changes in emissions and climate change?
5. How do the historical and projected changes in Hg air concentration and deposition relate to changes in mercury levels in other environmental compartments and biota?
6. How well can we represent the processes that affect the long-term changes of Hg levels and fluxes in quantitative models?
7. What efforts are needed to develop a system of observations, emissions, and models to better understand and track these changes?

A program of multi-model assessment and attribution of long-term Hg pollution trends in the EMEP and other regions was proposed at the workshop. The objectives of the assessment include retrospective analysis of Hg pollution changes based on model estimates and measurement data, attribution of Hg concentration and deposition trends to regional and extra-regional anthropogenic emissions, analysis of other factors affecting long-term Hg pollution changes, as well as projection of future levels of Hg atmospheric pollution based on emission scenarios. A number of scientific groups from various institutions of Europe and North America agreed to take part in the study with their Hg chemical transport and box multi-media models. Pilot results of a model assessment of Hg pollution trends and their attribution to various factors (changes in anthropogenic emissions, meteorological conditions, atmospheric chemistry, land cover etc.) were shown to illustrate possible outcome of the study and input data required.

A number of limitations and uncertainties associated with the proposed assessment of Hg pollution trends were indicated and discussed by the workshop participants. It was mentioned that assessment of long-term (decades) Hg historical trends and future projections should take into account changes in secondary Hg emissions and legacy Hg accumulated in the environmental reservoirs. In particular, ignoring changes in legacy emissions can lead to substantial errors and misleading policy conclusions. Since majority of atmospheric chemical transport models does not account for the Hg cycling among and accumulation in the environmental media, several simplified approaches were suggested to take into account the effect of legacy emissions dynamics. Besides, it was proposed to split the assessment into two phases, with the first phase to be focused on a study of the atmosphere-terrain and atmosphere-ocean exchange fluxes under contemporary conditions involving limited measurement data on Hg air-surface exchange. Results of the first phase should be used for attribution of Hg pollution trends at the second phase of the study.

Needs and availability of input data required for the assessment, which include emissions inventories and measurements, were also discussed. It was indicated that there are a number of existing global spatially distributed Hg emission inventories for long time periods, as well as future projections. However, the available inventories contain significant uncertainties in terms of consistency of time series and inter-comparability among the datasets. Therefore, additional efforts to update and improve the global Hg emissions inventories are needed. Measurement data on Hg air concentration and wet deposition were reported from various global and regional monitoring networks (EMEP, GMOS, NADP/MDN, AMNet, etc.) Available datasets cover significant time periods and will be available for trend analysis in the forthcoming multi-model assessment.

Discussion at the workshop and the following meeting of the co-ordination group allows identifying near-term (within two years) and longer-term programs of Hg activities within TF HTAP. The near-term activities (2022-2023) will include co-operative development/update of a global inventory of contemporary and historical Hg emissions, compilation of available measurement data from ground-based monitoring networks and measurement campaigns for the current and historical periods, and multi-model simulations of Hg contemporary dispersion and cycling on a global scale with focus on air-surface exchange, secondary/natural emissions.

The longer-term activities (2024-2026) will consist of development of future Hg emission scenarios, simulation and analysis of historical trends of Hg deposition, trends attribution to changes in regional and extra-regional emissions and other factors, and multi-model projections of future Hg pollution in the EMEP and other regions.

2.2. Workshop on POPs

The Workshop on POPs was attended by 81 experts from various countries and international organizations. The main purpose of the workshop was to initiate cooperative research activities that will enable TF HTAP to better contribute to a possible future review of the effectiveness and sufficiency of the POPs Protocol of the Air Convention. In particular, to better assess the regional and extra-regional contribution to long term trends in POPs and to identify additional issues or measures that might be addressed by the Air Convention to protect the environment and human health.

A preliminary list of policy-relevant science questions, prepared to support future co-operative activities on POPs and CEC, was presented by the TF HTAP chairs:

1. What are the observed and modelled trends in air concentration and deposition of POPs/CEC in the UNECE region and other regions of the globe?
2. To what extent are these trends associated with emission changes within each region or dependent on transport between regions and other environmental factors?
3. What are the relative contributions of contemporary and legacy emission sources to POPs/CEC concentrations and deposition in various regions and how have they changed over time?
4. How may POPs/CEC air concentrations and deposition levels and the contribution of various sources change in the future due to changes in emissions and climate change?
5. How do the historical and projected changes in POPs/CEC air concentrations and deposition relate to changes in levels in other environmental compartments, biota, or humans?
6. How well can we represent the processes that affect the long-term changes of POPs/CEC levels and fluxes in quantitative models?
7. What efforts are needed to develop a system of observations, emissions, and models to better understand and track these changes?

Participants of the workshop were informed about the outcome of recent assessments devoted to POPs compiled under the Stockholm Convention and AMAP. In particular, analysis of long-term trends for the wide range of POPs/CEC in abiotic and biotic environments was presented. Besides, recent

studies of POP/CEC long-range transport and effects of climate change on POPs distribution and fate were outlined along with information on the knowledge gaps and research needs. Furthermore, it was noted that polycyclic aromatic hydrocarbons (PAHs) were not included under the Stockholm Convention but represent an important topic for the analysis under the Air Convention. Although there are continuing concerns about legacy POPs that have been banned or restricted, there was general consensus that it would be reasonable to focus further co-operative research activities on continuing sources of POPs associated with combustion and CEC.

Similar to the Hg workshop, a number of existing and being developed global spatially distributed POP emission inventories for both historical and current periods, as well as future projections were presented. The workshop participants noted the opportunity to reconcile the differences between existing emissions inventories and to integrate combustion-related POPs into emissions inventories and scenarios developed for more traditional air pollutant emissions (e.g., HTAPv3).

In addition, the need to better integrate the significant work under the Convention on particulate matter, and condensables with the work on combustion-related POPs (e.g. PAHs, PCDD/Fs) was emphasized. The participants identified the opportunity to build upon the ongoing TFMM EuroDelta-Carb multi-model assessment of B(a)P pollution in Europe and extend it with the comparison to a larger number of global models and potentially to other combustion-related POPs.

Finally, participants expressed a strong interest in establishing a forum or another mechanism to maintain communication and collaboration across the POPs scientific community based on dedicated list servers, quarterly webinars, and data sharing sites.

3. Pilot analysis and attribution of long-term Hg and POP pollution trends

Attribution of long-term pollution trends is considered as one of the perspective directions of TF HTAP future activities on heavy metals and POPs. Proposed objectives of such research include retrospective analysis of the pollution changes, attribution of the trends to various factors (primary and secondary emissions, meteorology, chemistry, land cover, sea ice extent etc.), projection of future levels based on emission scenarios. To facilitate the discussion and reveal possible issues and uncertainties of the research pilot simulations of Hg and selected POPs were performed. Preliminary results of the study are briefly discussed below.

3.1. Model setup and experiments

Long-term simulations of Hg and POP levels as well as trend attribution experiments were carried out using the updated GLEMOS model. Description of the current stable model version 2.2.1 is available at the MSC-E website (<http://en.msceast.org/index.php/j-stuff/glemos>). The model updates include implementation of new input data on air concentrations of chemical reactants for a long period generated by the GEOS-Chem model [Travnikov *et al.*, 2020] and multi-year land cover data [Ilyin *et al.*, 2021]. More detailed description of input information used in the modelling (emissions, meteorological fields, chemical reactants, and land cover) is given in Section 3.2.

The simulations of Hg and two PAHs – benzo(a)pyrene (B(a)P) and fluoranthene (FLA) – were performed on a global scale with the spatial resolution 3°×3° for the period 1990-2018. Time series of simulation results were evaluated against available measurement data. Emission sources tagged simulations were conducted to estimate source-receptor relationships of Hg and PAHs air concentration and deposition in terms of global source regions (Fig. 1). The definition of the sources regions follows specifications adopted within the HTAP2 Experiments (<http://iek8wikis.iek.fz-juelich.de/HTAPWiki/WP2.1>).

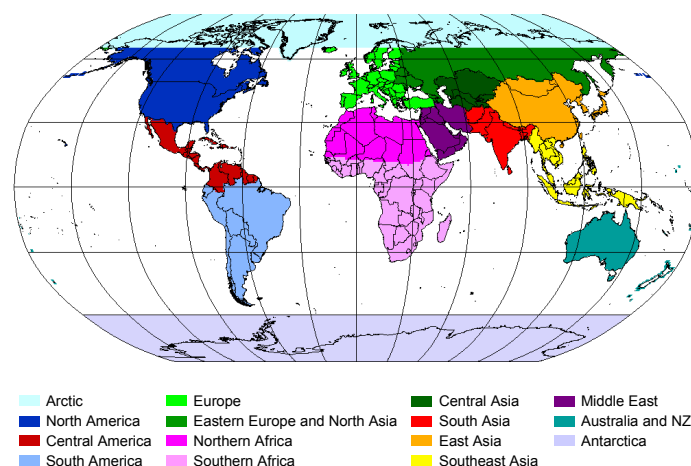


Fig. 1. Definition of source and receptor regions used in the study.

Additionally, a number of the model sensitivity runs were carried out to evaluate influence of several anthropogenic and environmental factors (emissions, meteorological conditions, atmospheric content of major chemical reactants, land cover distribution) on long-term changes of Hg and POP levels in various regions of the globe. The whole list of the model experiments is given in Table 1.

Table 1. List of the model sensitivity experiments.

Code	Purpose	Description
BASE	Full trend calculation	Base model run for the period 1990-2018
EMIS	Evaluation of emission change effect	The same as BASE but with anthropogenic emissions fixed at 1990 year
METEO	Evaluation of meteorol. conditions change effect	The same as BASE but with meteorological data fixed at 1990 year
CHEM	Evaluation of atmospheric chemistry change effect	The same as BASE but with concentration of chemical reactants fixed at 1990 year
LCOV	Evaluation of land cover change effect	The same as BASE but with land cover fixed at 1990 year ^(*)

(*) Since the data on long-term changes of land cover are available for the shorter period (2001-2018), the land cover distribution of 2001 was used unchanged for the preceding period 1990-2000.

The base run (BASE) was performed with the state-of-the-art model formulation for the whole period 1990-2018. The year 1990 was chosen as the reference year for the following study. Preliminary analysis of the meteorological conditions in 1990 did not reveal significant deviation them from the average conditions of the whole period. A number of sensitivity tests (EMIS, METEO, CHEM, LCOV) were performed with values of the selected parameters fixed as of the year 1990 to evaluate the effect of temporal variation of the parameters on changes of the pollutant levels over the period. Then simulation results of the tests were compared with those of the base run. To quantify relative contribution of the parameters to the whole changes of the pollution levels the following characteristic was calculated

$$\varepsilon_Y^f = \frac{X_Y^{base} - X_Y^f}{X_{1990}^{base}} \cdot 100\% ,$$

where X_Y^{base} and X_{1990}^{base} are values of the pollution characteristics (air concentration or deposition flux) simulated in the base run for years Y and 1990, respectively; X_Y^f is the value of the pollution characteristics in year Y according to the sensitivity run f (EMIS, METEO, CHEM, LCOV). The total relative change of the characteristics with respect to 1990 is calculated as follows

$$\varepsilon_Y = \frac{X_Y^{base} - X_{1990}^{base}}{X_{1990}^{base}} \cdot 100\% .$$

The effect of unaccounted factors on changes of the pollution levels is calculated as a difference between the total relative change and the sum of relative changes due to individual factors

$$\varepsilon_Y^{other} = \varepsilon_Y - \sum_f \varepsilon_Y^f .$$

Mentioned above characteristics are used in the analysis presented hereafter in Sections 3.3 and 3.4.

3.2. Input data

Meteorological conditions, atmospheric concentrations of some chemically active substances, land cover characteristics as well as anthropogenic and natural/secondary emissions are the factors, which can possibly affect changes in concentration and deposition levels of Hg and POPs in the atmosphere. Time-series of these factors used in the study are described below.

3.2.1. Meteorological data

Meteorological information for 1990-2018 time period has been generated from the ERA-Interim reanalysis data of the European Centre for Medium Range Weather Forecasts [ECMWF, 2020] using the meteorological pre-processor based on the Weather Research and Forecast modelling system (WRF) [Skamarock et al., 2008]. The pre-processed precipitation data were additionally corrected using the GPCP Version 2.3 Combined Precipitation Data Set [Adler et al., 2003]. Time-series of annual precipitation and temperature levels averaged over the selected TF HTAP regions are presented in Figs. 1 and 2, respectively.

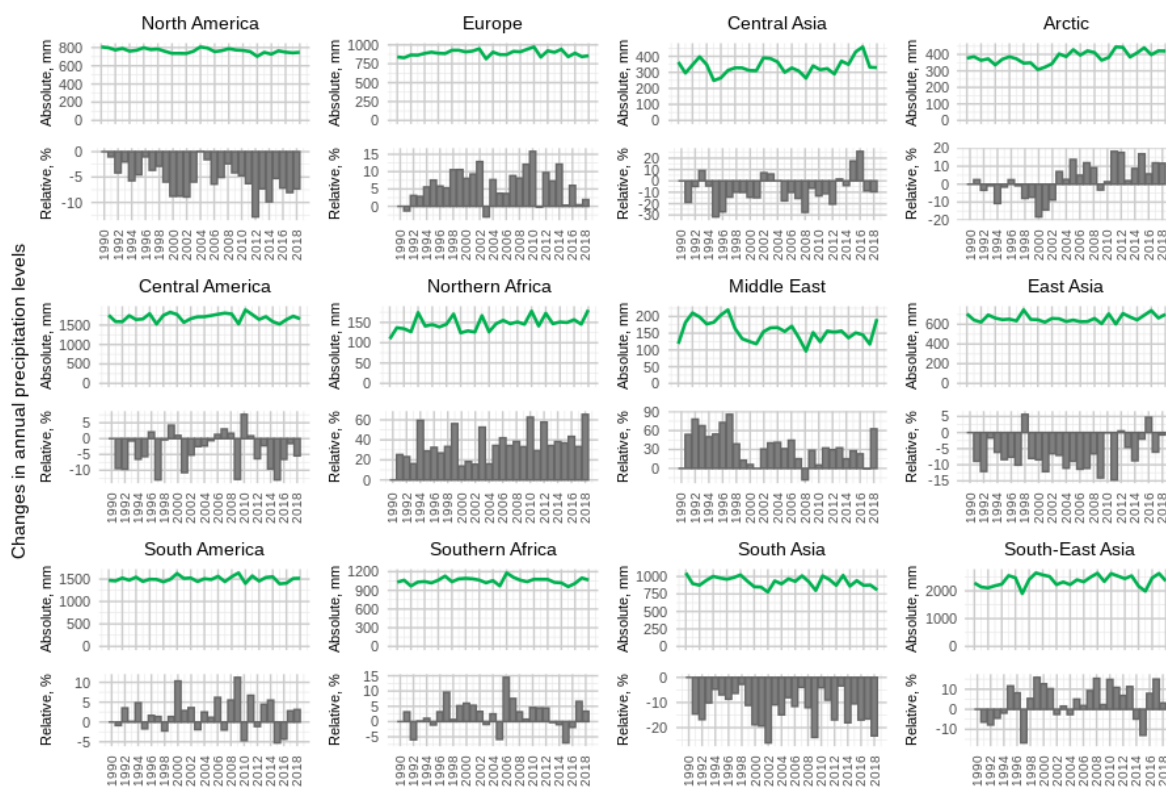


Fig. 1. Long-term absolute and relative changes of annual precipitation amounts in various regions over the period 1990-2018.

According to the data, in general, annual precipitation amounts can vary significantly from one year to another in every region (Fig. 1). The data shows a slight downward trend in North America from 2004 to the present. In the Arctic, the precipitation levels were decreasing from 1995 to 2000 by 20%, then significantly increased by 2011 and then decreased again by 2018. In addition, in regions with dry climates, such as the Middle East and Northern Africa, enormous relative changes can be explained by

generally low absolute values of precipitation amounts. At the same time, it is noticeable that over the 29-year period, the air temperature in most regions grew. (Fig. 2). Since 1990, the annual mean temperature has increased by 1° in the European region as well as by 2° in the Arctic. Similarly, the temperature has increased by 0.5° over North America. In other regions the annual mean air temperature increased insignificantly over the period.

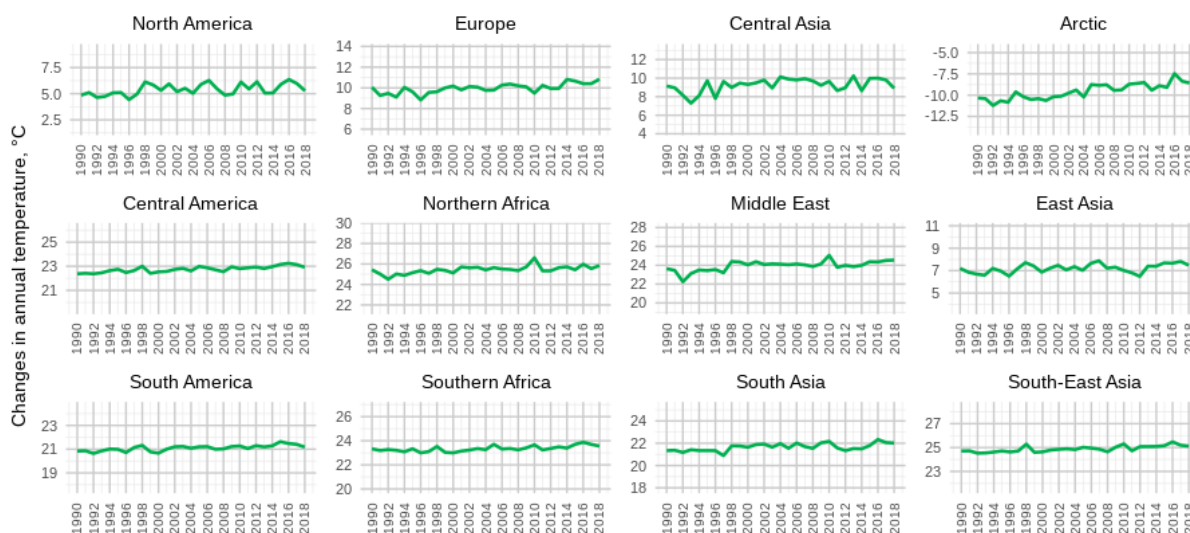


Fig. 2. Long-term changes of annual mean near-surface air temperature in various regions over the period 1990-2018.

3.2.2. Chemical reactants

Required atmospheric concentrations of chemical reactants, namely ozone (O₃), hydroxyl radical (OH), black carbon (BC), organic carbon (OC) and particulate matter (PM_{2.5}) were calculated using the GEOS-Chem model (version 12.8.2). The standard full-chemistry simulation from 1990 to 2018 has been carried out on the 4°×5° horizontal grid. Before calculation the model had been spun up using the data for 1989. The simulated 3D concentration fields of all the reactants were interpolated to the GLEMOS native grid.

In most of TF HTAP regions the GEOS-Chem modelling results show insignificant ozone concentration changes. However, there are noticeable increasing trends in the Middle East, South Asia and Central America. Annual ozone concentrations in these regions rose by 10% from 1990 to 2018. It can be seen that OH concentrations considerably increased from 1990 to 2008 over Central America as well as in the Middle East and in South Asia over the whole period. At the same time, a 10% decreasing trend of OH concentration over North America can be noticed.

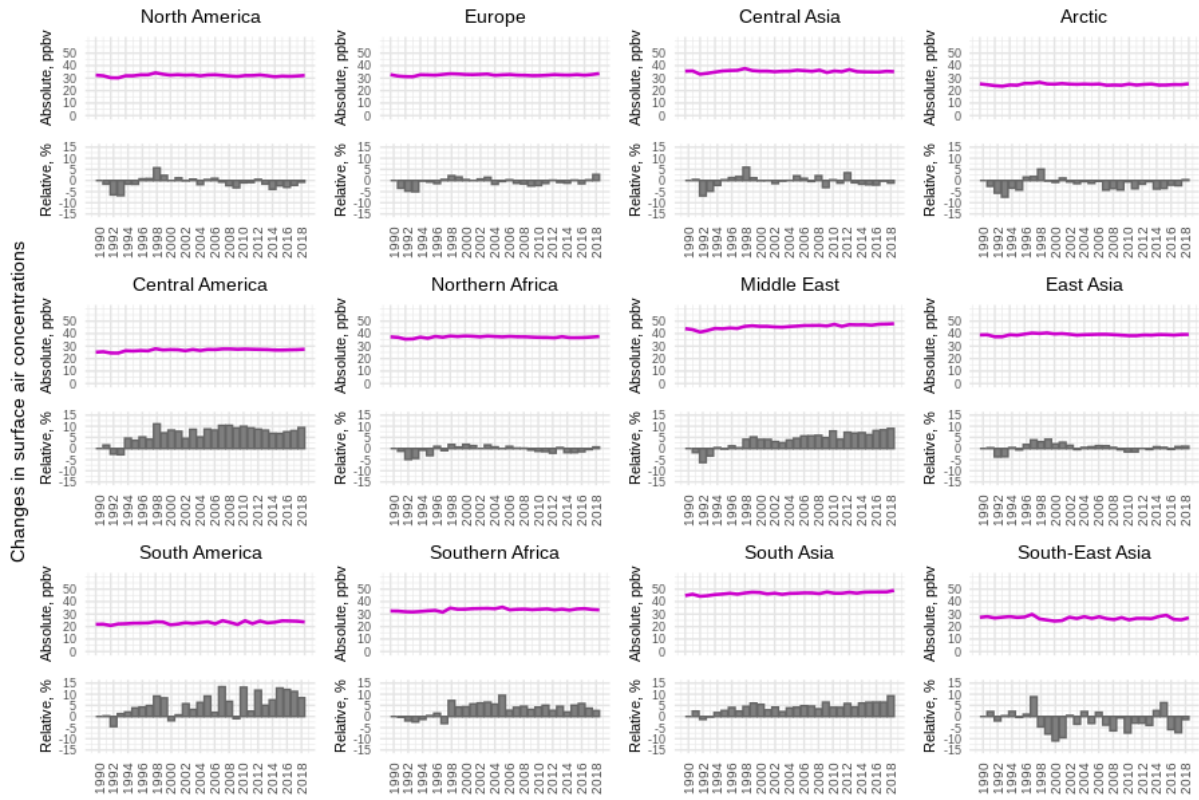


Fig. 3. Long-term absolute and relative changes of annual mean near-surface ozone air concentration in various regions over the period 1990-2018.

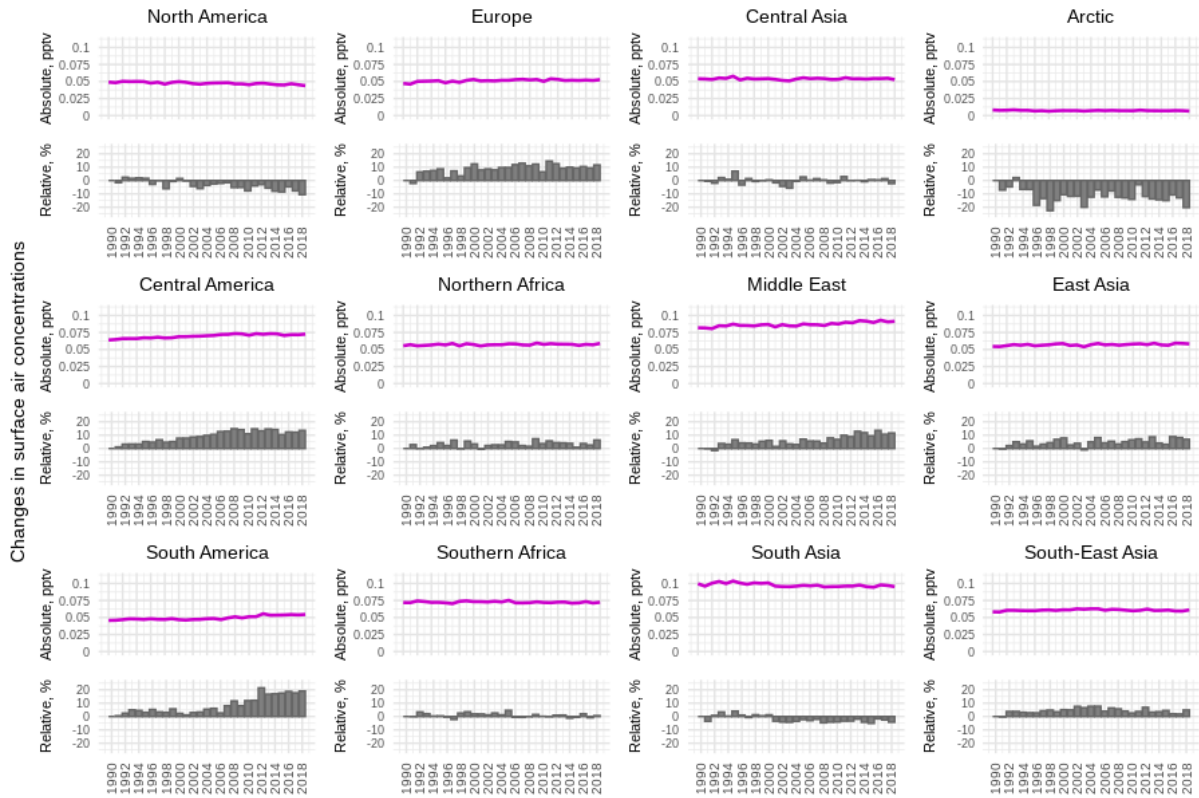


Fig 4. Long-term absolute and relative changes of annual mean near-surface hydroxyl radical air concentration in various regions over the period 1990-2018.

3.2.3. Land cover

Information on long-term changes in the surface conditions was obtained from the Terra and Aqua combined Moderate Resolution Imaging Spectroradiometer (MODIS) Land Cover data product (MCD12Q1, version 6) [Friedl *et al.*, 2019]. This product provides global distribution of land cover types at yearly intervals (2001-2018) with 500-m spatial resolution. For the sake of compatibility with the model parameterizations the data product layer derived from the International Geosphere-Biosphere Programme (IGBP) classification was utilized. Fixed land cover distribution for 2001 was used for the period 1990-2000, which is not covered by the data product.

Absolute and relative changes in the area of some land cover types in various regions are shown in Figs. 5 and 6. There are continuous decreasing trends in the forest area in several regions over the period 2001-2018: -5% in South America, -1% in North America, almost -2% in Southern Africa starting from 2011 and the same in the Middle East starting from 2016 (Fig. 5). Along with this trend in all the regions, excluding the Middle East, there is a tendency towards increasing area of arable lands, especially in South America - more than 20% over the 18-years period (Fig. 6). Continuous increase in the forest area is visible in both East and South Asia. In the European region there is a decrease of the forest area from 2001 to 2003 and further growth by 2016. In addition, in all regions there is a strong tendency towards increase of the area of urban and built-up lands and simultaneous decrease of barren lands (excluding the regions with arid climate such as the Middle East and Central Asia, where the area of barren lands is relatively stable throughout the whole period).

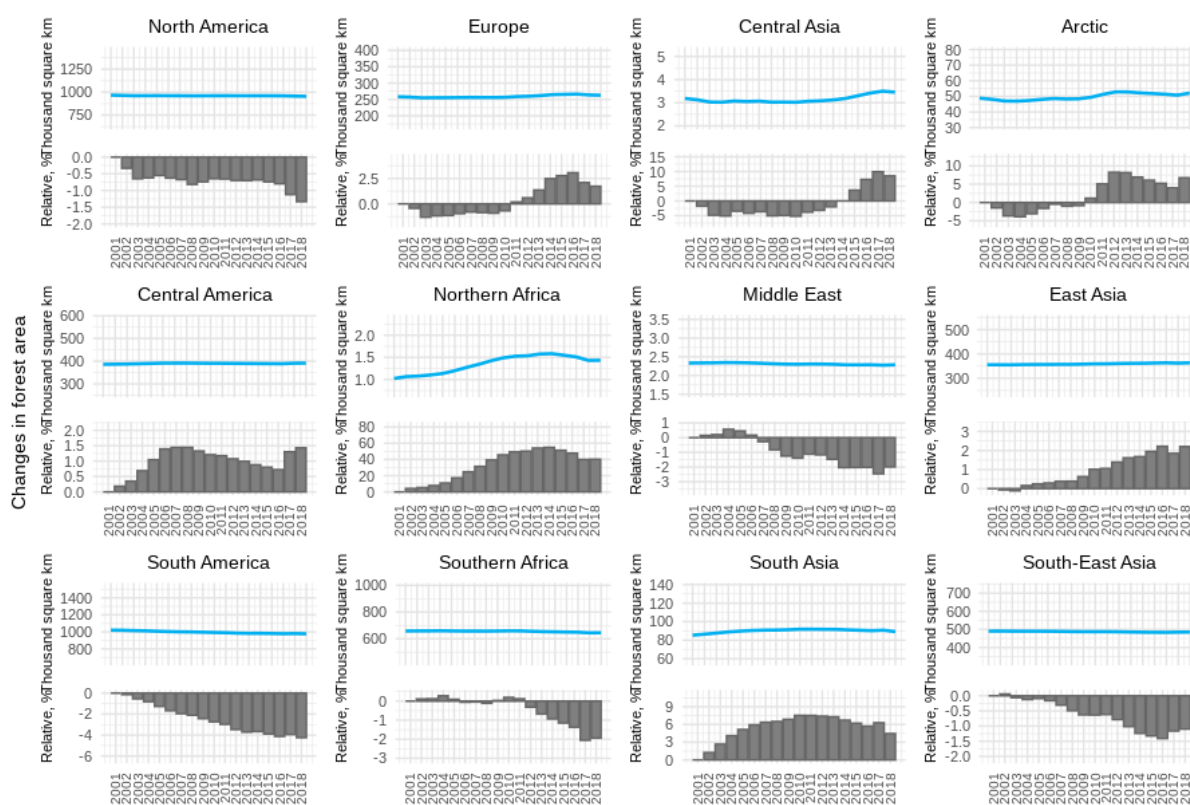


Fig. 5. Long-term absolute and relative changes of forest area in various regions over the period 1990-2018.

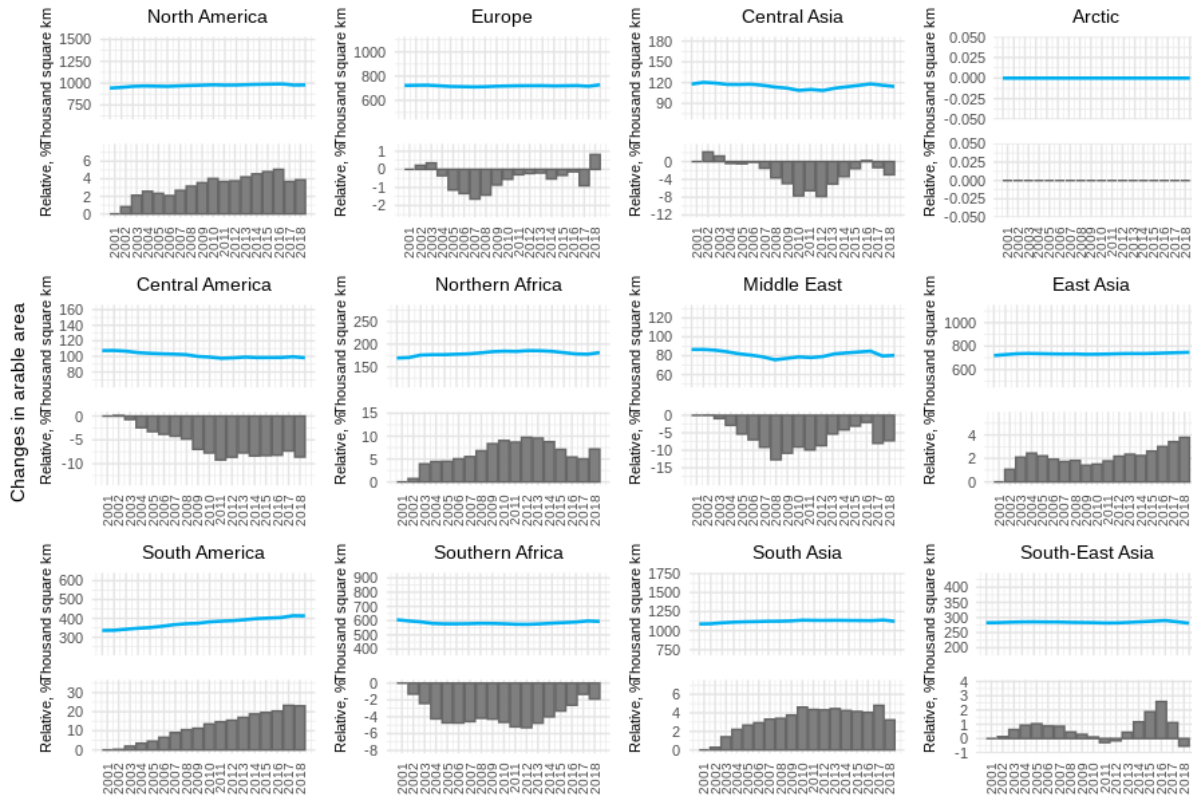


Fig. 6. Long-term absolute and relative changes of arable lands area in various regions over the period 1990-2018.

3.2.4. Emissions

There are a few global emissions inventories for Hg, which cover the considered time period 1990-2018. They include the global inventories from two UNEP Global Mercury Assessments – GMA 2013 [AMAP/UNEP, 2013] and GMA 2018 [AMAP/UNEP, 2019]; the global dataset from the EDGARv4.tox2 database [Muntean et al., 2018] and the long-term emissions estimates by Streets et al. [2019a; 2019b]. The first two inventories are spatially resolved, whereas the third one consists of total emission estimates for various regions of the globe. The GMA 2013 (1990, 1995, 2000, and 2005) and GMA 2018 (2010 and 2015) datasets present consistent datasets for selected years but not consistent with each other because of different applied methodologies. The EDGAR inventory covers the period 1970-2012 with self-consistent emissions data. The dataset by Streets et al. presents estimates of Hg emission changes from preindustrial times (1510) to the present day (2010) with the decadal time step [Streets et al., 2019a] and the annual emissions estimates for the recent years 2010-2015 [Streets et al., 2019b].

Figure 7 shows comparison of Hg emission estimates from these inventories both on a global scale and for particular regions. As seen the global estimates differ considerably between the inventories, particularly, at the beginning of the period (Fig. 7a). The GMA and Streets’ inventories relatively well agree with each other, whereas the EDGAR dataset provides considerably lower estimates. The difference is even more pronounced for some regions – Europe and East Asia (Figs. 7b and 7d). Besides, the inconsistency between the GMA 2013 and GMA 2018 datasets is well seen for emissions in East Asia (Fig. 7d).

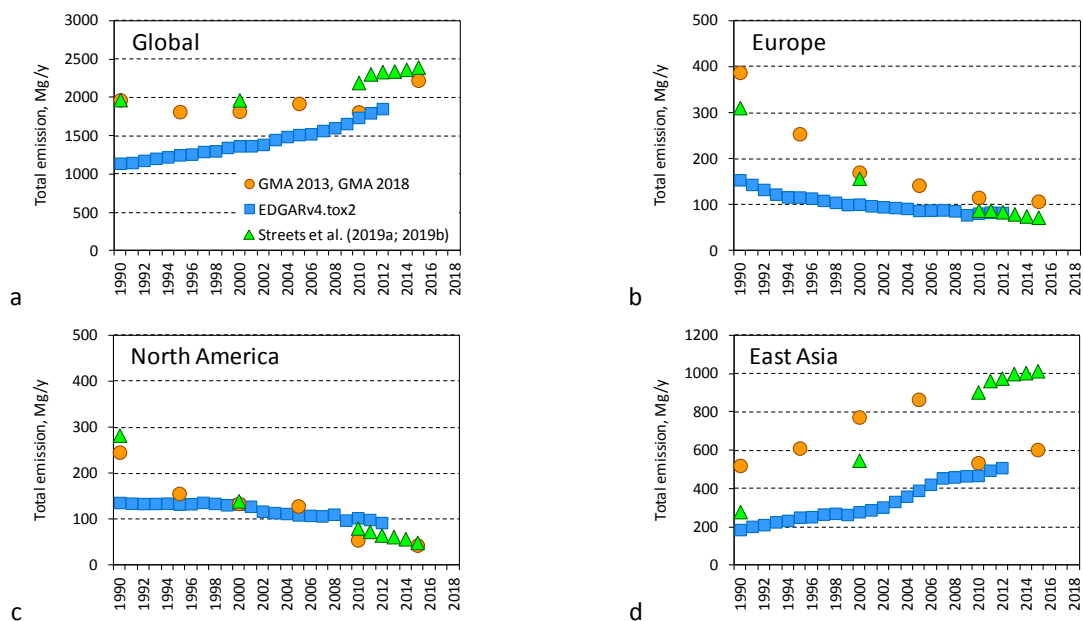


Fig. 7. Long-term changes of Hg anthropogenic emission: (a) – global; (b) – in Europe; (c) – in North America; (d) – in East Asia. Circles show estimates from GMA 2013 (AMAP/UNEP, 2013) and GMA 2018 [AMAP/UNEP, 2019], squares – from EDGARv4.tox2 [Muntean et al., 2018], triangles – from Streets et al. [2019a; 2019b].

To generate a consistent Hg emissions dataset for the period 1990–2018 we combined the GMA and Streets’ inventories using the spatial distributions of emissions in various regions of the globe from the former and total emission values for the regions from the latter. Emission gaps for the years not covered by the Streets’ inventory were filled using linear interpolation between the nearest years. Figure 8 shows the resulting Hg emissions maps for the years 1990 and 2018. As seen, there is pronounced emissions reduction in Europe and North America as well as emissions growth in East Asia.

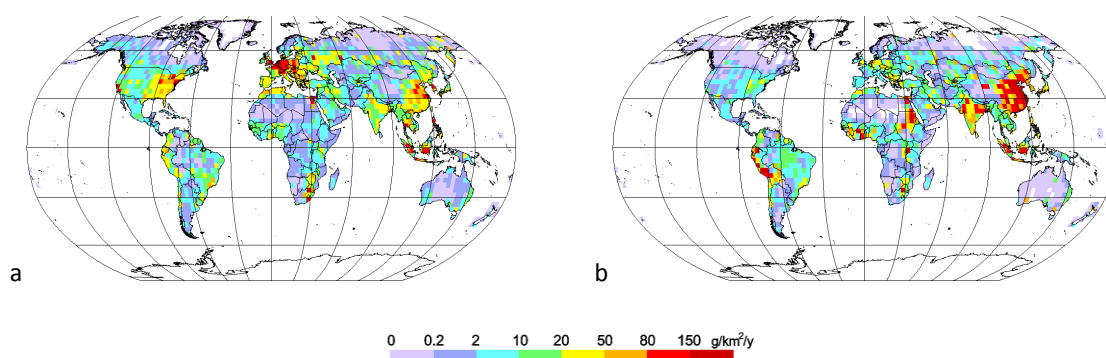


Fig. 8. Spatial distribution of global annual Hg emission in 1990 (a) and 2018 (b).

Temporal changes of estimated Hg anthropogenic emissions from 1990 to 2018 are shown in Fig. 9. Emissions reduction in Europe and North America was more significant during the first decade of the period and then became more gradual until 2014 declining overall by 80% in both regions. In contrast, Hg emission increased significantly in East and South Asia, South America, and Africa. In the Arctic, Hg emission decreased by 60% from 1990 to 2000, but then the reduction changed by some growth. Similarly, in Central America and the Middle East there was a smooth decreasing trend from 1990 to 2011 followed by growth through 2015.

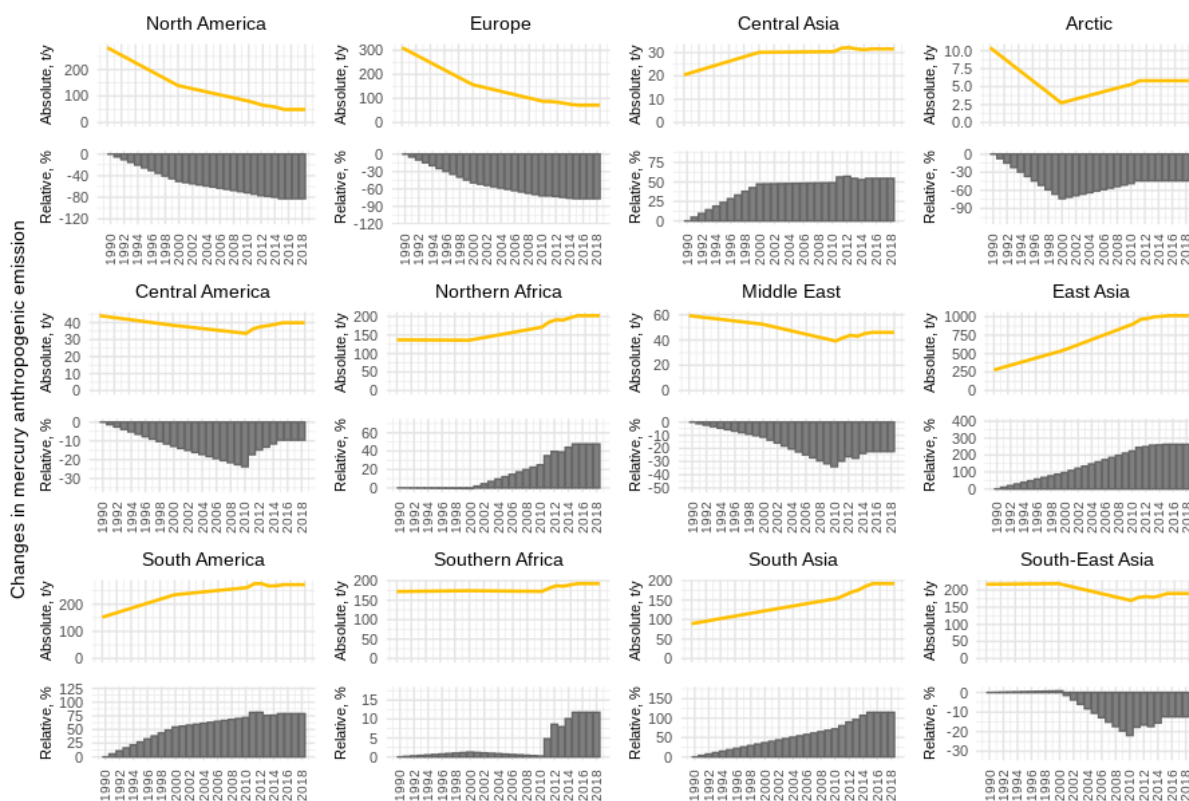


Fig. 9. Long-term absolute and relative changes of anthropogenic Hg emissions in various regions over the period 1990-2018.

Prescribed fluxes of natural and secondary Hg emissions from soil and seawater were generated depending on Hg concentration in soil, soil temperature and solar radiation for emissions from land and proportional to the primary production of organic carbon in seawater for emissions from the ocean [Travnikov and Ilyin, 2009]. The total values of global Hg natural/secondary emissions were scaled to fit the temporal dynamics of measured Hg^0 concentrations worldwide over the period 1990-2018. Additionally, prompt re-emission of Hg from snow is taken into account using an empirical parameterization based on the observational data [Kirk et al., 2006; Johnson et al., 2008; Ferrari et al., 2008].

Global datasets of benzo(a)pyrene (B(a)P) and fluoranthene (FLA) atmospheric emissions were derived from the global emissions inventory for 16 PAHs developed by the research group of Peking University [Shen et al., 2013]. The inventory is based on a top-down approach with application of the newly developed fuel consumption database PKU-FUEL-2007 [Wang et al., 2013] and an updated database of PAH emission factors. In addition to these two substances, the inventory also includes information on global emission of naphthalene (NAP), acenaphthylene (ACY), acenaphthene (ACE), fluorene (FLO), phenanthrene (PHE), anthracene (ANT), pyrene (PYR), benzo(a)anthracene (B(a)A), chrysene (CHR), benzo(b)fluoranthene (B(b)F), benzo(k)fluoranthene (B(k)F), dibenzo(a,h)anthracene (D(ah)A), indeno(1,2,3-cd)pyrene (I(cd)P), and benzo(g,h,i)perylene (B(g,h,i)P). Spatial distribution of annual emissions of 16 PAH for 2014 is given in Fig. 10. According to these data, the highest level of PAH emissions took place in the countries of East and South Asia.

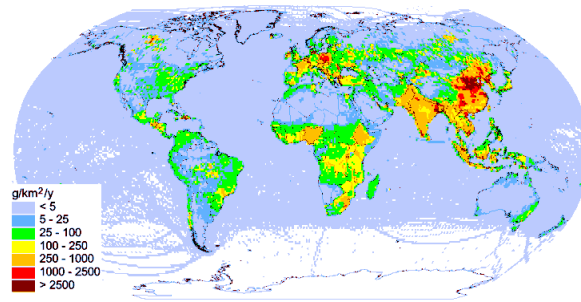


Fig 10. Spatial distribution of global annual emissions of 16 PAHs for 2014.

In Europe, North America, and Central Asia the total decline of B(a)P ranged from 60% to 80% over the period, which was more rapid from 1990 to 2000 and more gradual by 2010 (Figs. 11 and 12). Data on FLA emissions show the maximum 40% growth in South Asia, whereas the highest B(a)P emission increase by 5-10% took place in South Asia and Southern Africa. However, it should be noted that emissions of both PAHs show very strong yearly fluctuations in some regions, especially in the Arctic, and South America.

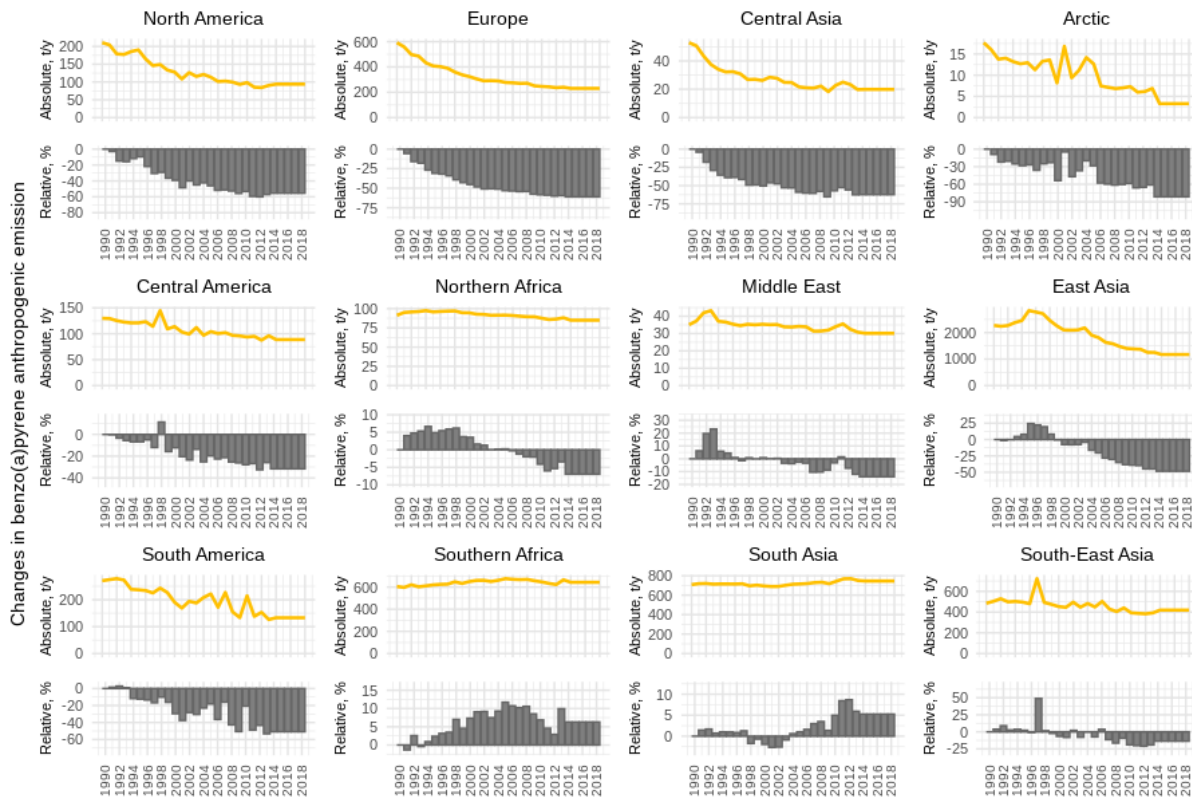


Fig. 11. Long-term absolute and relative changes of anthropogenic B(a)P emissions in various regions over the period 1990-2018.

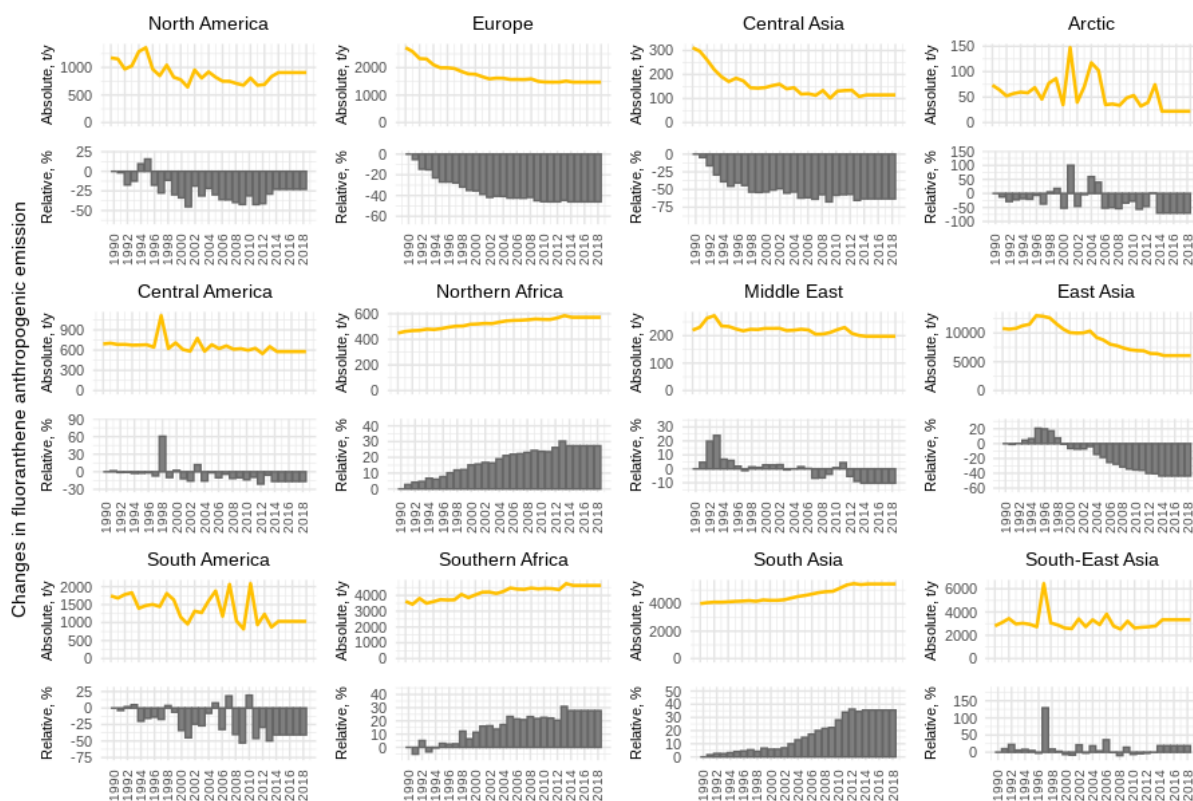


Fig. 12. Long-term absolute and relative changes of anthropogenic FLA emissions in various regions over the period 1990-2018.

3.3. Long-term changes of Hg pollution

Long-term changes of Hg pollution levels on a global scale were simulated using emissions data and other model input information described in Section 3.2. The modelling results were evaluated against limited set of measurement data. The measurement dataset is largely based on the long-term observations from the EMEP monitoring network in Europe and the NADP/MDN network in North America. In addition, a global collection of Hg measurements in air and precipitation in 2013 was involved from [Travnikov *et al.*, 2017] to characterize spatial distribution of Hg levels on a global scale.

The model simulations cover the period 1990-2018 and characterize temporal changes of Hg air concentration and deposition in different regions. Figure 13 shows simulated distributions of Hg⁰ concentrations for selected years of the considered period (1990, 2000, 2010, 2018). As seen the most significant changes of the global concentration pattern took place between 1990 and 2000 (Figs. 13a and b). Concentration levels declined considerably in Europe and North America but increased in East Asia. Emissions reduction in major source regions and long residence time of Hg⁰ in the atmosphere leads to general decrease of background Hg⁰ levels in the Northern Hemisphere. The concentration further decreased between 2000 and 2010 in Europe and increased in East Asia (Fig. 13c). The changes of Hg⁰ concentration during the last decade of the period (2010-2018) were insignificant (Fig. 13d).

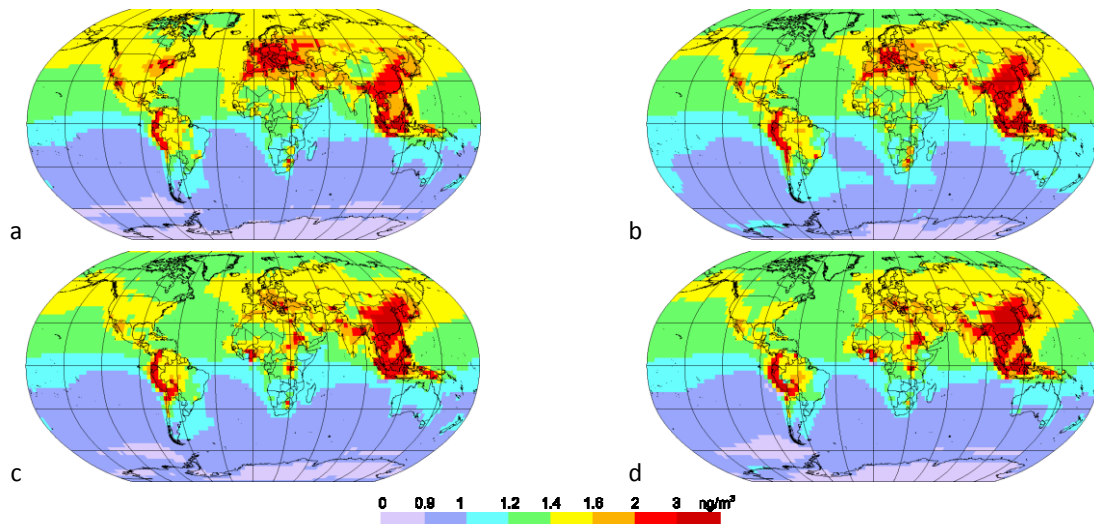


Fig. 13. Global distributions of Hg^0 air concentration in 1990 (a), 2000 (b), 2010 (c), 2018 (d).

Comparison of simulated global patterns of Hg air concentrations as well as Hg wet deposition with observations for 2013 is shown in Fig. 14. The model well reproduces general levels and spatial distribution of Hg^0 air concentration on a global scale (Fig. 14a). Elevated concentrations are predicted in industrial regions of Europe, North America, East, South and Southeast Asia, as well as in a number of regions in the tropics that are characterized by intensive artisanal and small-scale gold mining (ASGM). The modelling results mostly agree with the observations within a factor of 1.5 (Fig. 14c). However, the model tends to overpredict the observed values in East Asia, probably, due to overestimated emissions in this region.

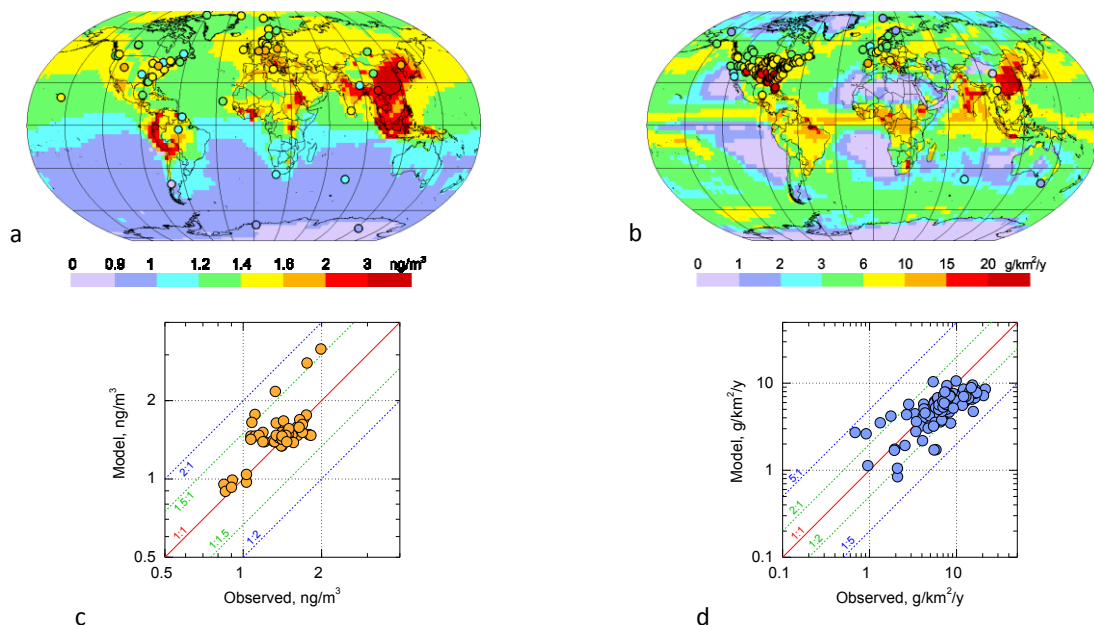


Fig. 14. Global distribution of Hg^0 concentration (a) and Hg wet deposition (b) in 2013. Circles show observed values in the same colour scale. Scatter plots show the model-measurement comparison for annual mean Hg^0 concentration (c) and Hg wet deposition (d). The measurement dataset is the same as in Travníkov et al. [2017].

The global pattern of Hg wet deposition reflects distribution of anthropogenic emissions and the spatial pattern of precipitation (Fig. 14b). The most significant fluxes are also characteristics of the industrial regions and the high-precipitation areas along the Intertropical Convergence Zone. The lowest deposition fluxes are simulated in the regions with low precipitation amounts – subtropical areas of the ocean, Northern Africa, Greenland and Antarctica. At the majority of the measurement sites the model-measurement deviation does not exceed a factor of 2 (Fig. 14d).

3.3.1. Observed and modelled temporal trends

Evaluation of simulated long-term changes of Hg^0 air concentration against available measurements in Europe and the Arctic is shown in Fig. 15. Both the model and observations show a significant decrease in Hg^0 concentration in Europe in since 1990 till 1997 and a levelling of the average concentration over the following period (Fig. 15a). This temporal dynamics is determined by various factors including changes of anthropogenic emissions in Europe and other regions as it will be shown below. Mercury concentrations in the European sector of the Arctic have not changed significantly since the mid-1990s as it follows from both the modelling and measurement data (Fig. 15b). This remote region is largely affected by long-range transport of Hg emissions from major source regions of the globe.

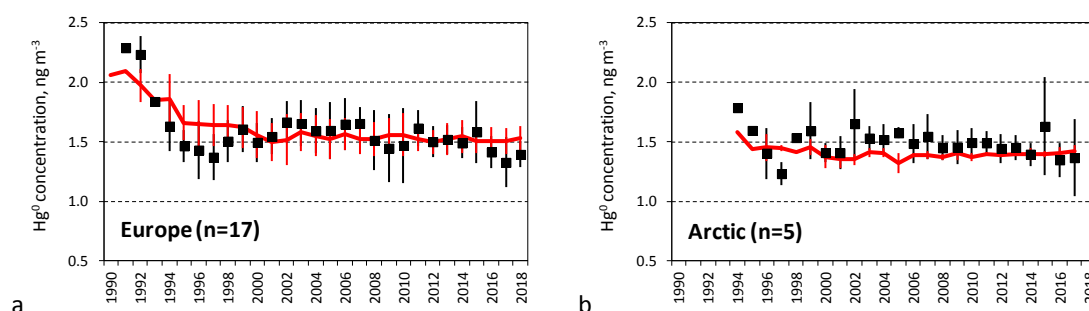


Fig. 15. Long-term changes of observed and modelled annual Hg^0 concentration in air at the EMEP monitoring sites in Europe (a) and the Arctic (b). Whiskers show standard deviation of measured and simulated values among the sites.

Mercury wet deposition is mostly formed by short-lived Hg species and, therefore, reflects regional changes of Hg emissions. Comparison of simulated and measured long-term variation of Hg wet deposition is shown in Fig. 16 for selected measurement sites in Europe and North America. As seen the model satisfactorily well reproduces both levels and seasonal variation of measurements in the available observational periods. The modelling results demonstrate considerable declining dynamics of Hg wet deposition during 1990s due to emission reduction in both regions. Since 2000, the long-term changes of Hg wet deposition have become insignificant and are largely masked by seasonal variation with maximum deposition in summer and minimum in winter.

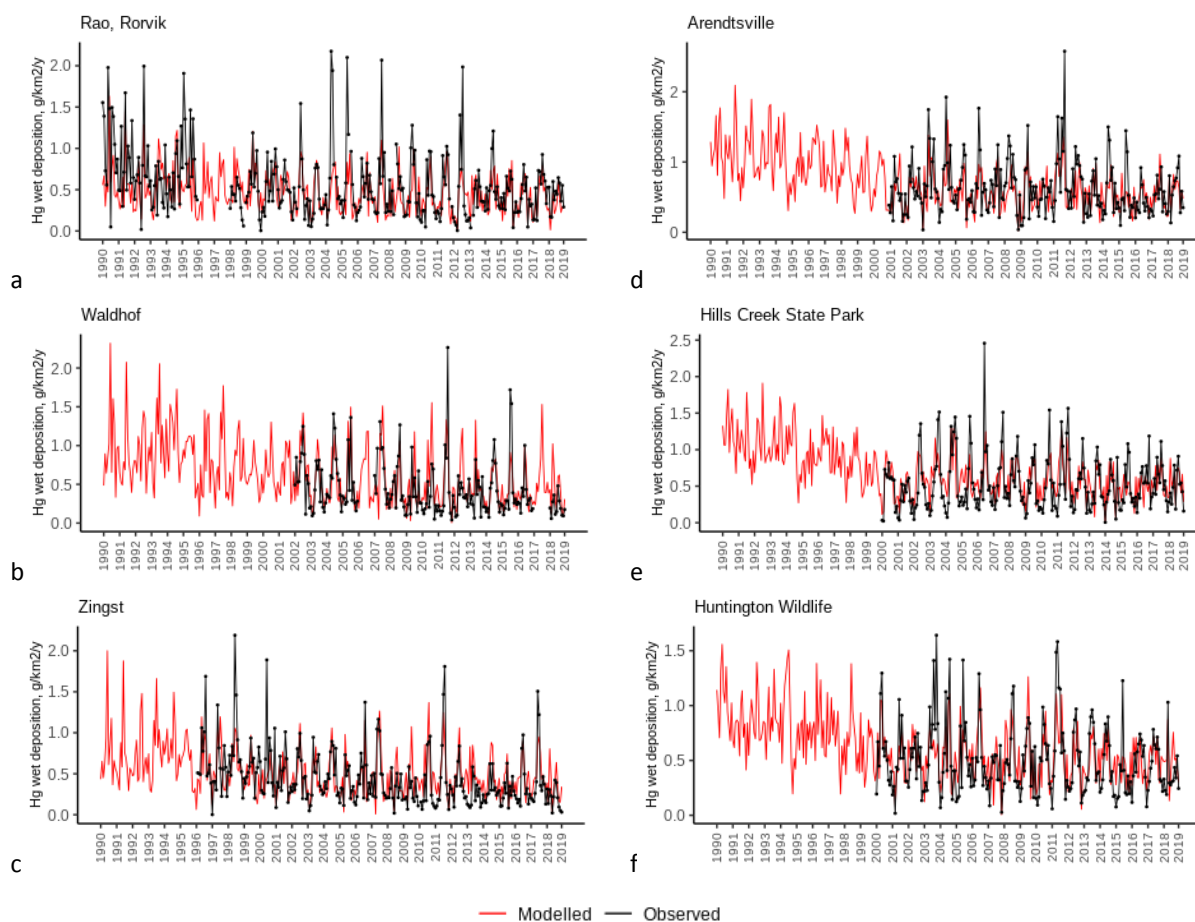


Fig. 16. Long-term changes of observed and modelled monthly Hg wet deposition at the EMEP sites Rao/Rorvik (a), Waldhof (b) and Zingst (c) in Europe, and the NADP/MDN sites Arendtsville (d), Hills Creek State Park (e) and Huntington Wildlife (f) in North America.

3.3.2. Trends attribution to regional and extra-regional emissions

One of the major factors affecting temporal changes of Hg concentration and deposition levels is changing of anthropogenic emissions as well as legacy/natural emissions in various regions of the globe. Long residence time of Hg in the atmosphere makes possible atmospheric transport of the pollutant over long distances and significant effect of the continents on each other. Therefore, the analysis of long-term changes of the pollution levels includes the trends attribution to regional and extra-regional emissions.

Figure 17 shows source apportionment of Hg⁰ air concentration trends in twelve selected regions (see definition of the regions in Section 3.1). As seen the dynamics of Hg⁰ concentration changes in Europe and North America is largely determined by decrease of contribution of regional sources due to emissions reduction in the regions, as well as by gradual increase of the contribution of East Asian emissions. Due to similar reasons, Hg⁰ levels do not change considerably over the whole period in the Arctic, where declining effect of long-range transport from North America and Europe has been compensated by growing contribution of East Asia. The growth of regional emissions in East Asia has led to considerable increase of Hg⁰ concentrations in the region (from 1990 to 2014) and has also affected pollution changes in most other regions. The contribution of legacy and natural emissions

gradually decreases over the period in all the regions. However, it should be mentioned that both the total estimates and temporal changes of this type of emissions contains significant uncertainties. In particular, in this pilot study the long-term changes of legacy/natural emissions were constrained by global measurements of Hg^0 concentration (Section 3.2) and, therefore, did not take into account real processes of Hg accumulation in the environmental media and the inter-media exchange.

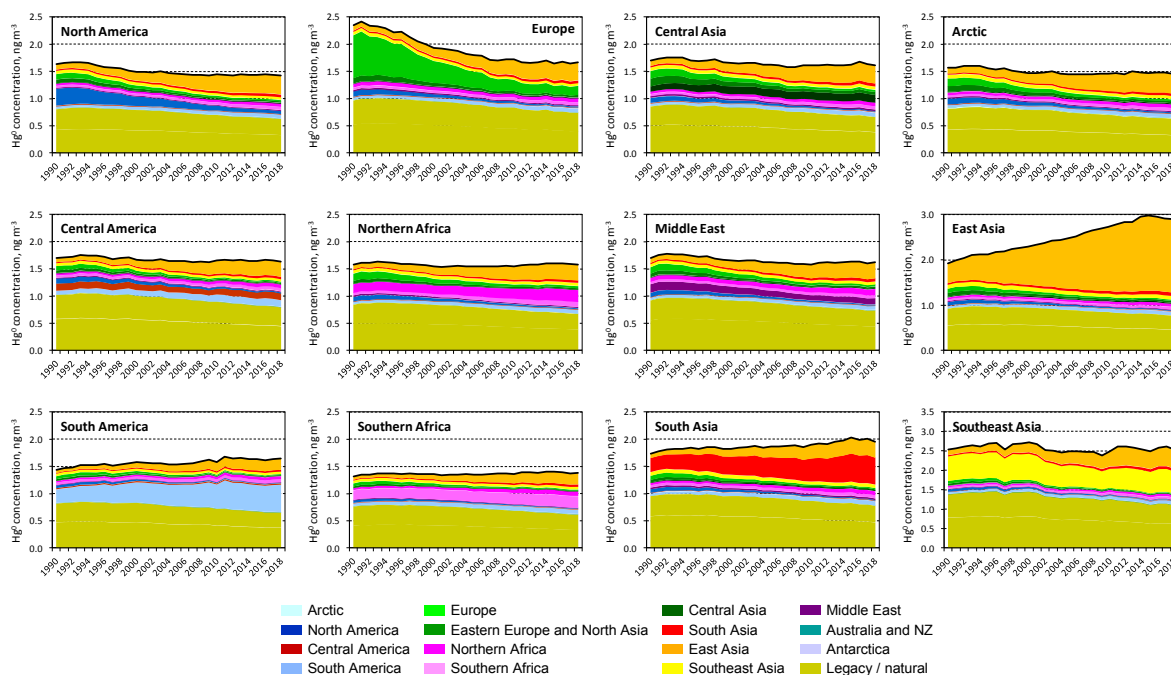


Fig. 17. Long-term changes and source apportionment of Hg^0 air concentration in various regions.

Thus, long-term changes of Hg levels in most regions of the globe are affected by changes of both regional and extra-regional anthropogenic emissions as well as secondary emissions of Hg accumulated in the environment. Estimates of historical and future trends of Hg pollution are sensitive to reliable data on global Hg emissions and their changes. Besides, estimates of Hg air-surface exchange leading to release of natural and legacy Hg from environmental media need to be further refined.

3.3.3. Trends attribution to environmental factors

Temporal variations of Hg pollution levels are also affected by various environmental factors that include, in addition to anthropogenic emissions, changes in the atmospheric and surface conditions, chemical composition of the atmosphere, biotic and abiotic processes in terrestrial and aquatic ecosystems etc. To analyze effects of the key factors on long-term changes of Hg concentration and deposition a number of sensitivity tests were carried out (Section 3.1). Results of the analysis are shown in Figs. 18 and 19 in terms of relative changes of Hg concentration and deposition, respectively, in various regions with regard to the year 1990.

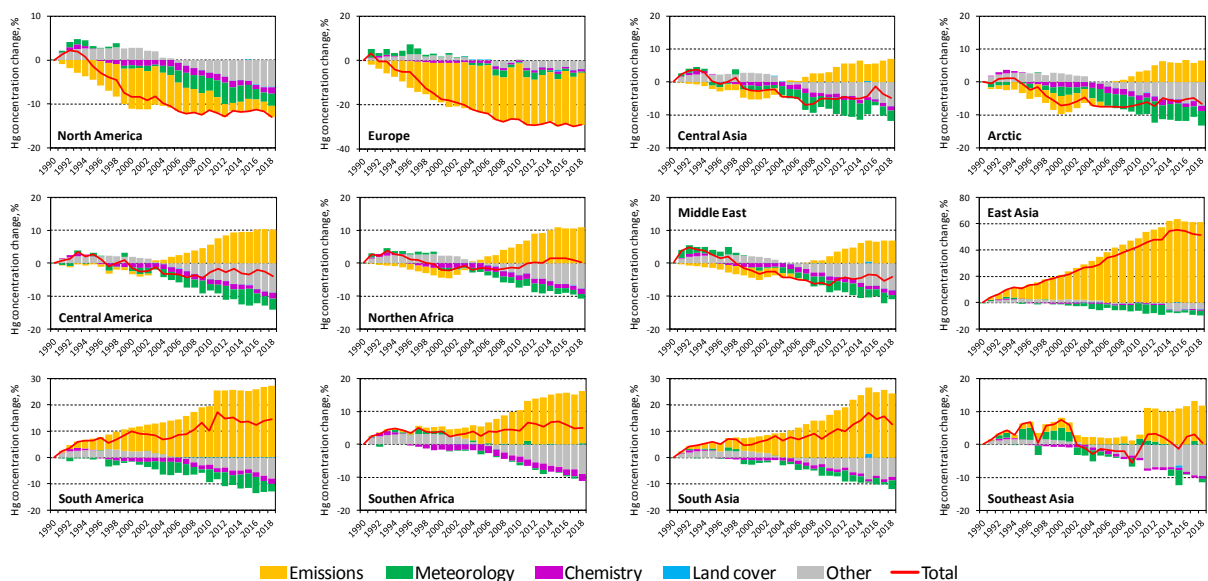


Fig. 18. Contribution of various factors to long-term relative changes of average Hg^0 air concentration in various regions. Red line depicts total cumulative change due to all factors.

The effect of changes in global anthropogenic emissions prevails over other factors in major industrial regions – Europe, North and South America, East and South Asia. However, the contribution of this factor changed over time. For instance, Hg^0 concentration decrease in North America from 1990 to 2000 was mostly determined by reduction of regional emissions. During the rest of the period, the contribution of emissions reduction declined because of increased transport of emissions from Asia. In some regions with small domestic emissions (e.g. the Arctic, Northern Africa, etc.) the effect of global emissions change altered over the period from reduction to growth reflecting emissions changes in the neighboring industrial regions.

The change in meteorological conditions led to insignificant (up to 5%) decrease of near-ground Hg^0 concentration in most considered regions. This effect can be connected with some increase of average air temperature (Section 3.2.1) that resulted in increased Hg^0 oxidation, and, probably, with increased vertical mixing of air masses in the atmospheric boundary layer. An additional decrease of Hg^0 concentration is caused by slight increase in chemical reactants (Section 3.2.2) participating in Hg transformations in the atmosphere. The effect of unaccounted factors mostly consists of changes in legacy/natural emissions and causes Hg^0 concentration decrease globally.

The effect of anthropogenic emissions is even more pronounced for long-term changes of Hg deposition in the regions with significant emissions (Fig. 19). It is caused by considerable contribution of domestic emissions of short-lived oxidized Hg species that deposit regionally. In contrast, the long-term changes of Hg deposition are more affected by variation of meteorological conditions, particularly, in regions with small domestic emissions (e.g. the Arctic, Central Asia, the Middle East, Central America, etc.). The influence of meteorological changes consists of a combined effect of increased air temperature leading to increased Hg^0 oxidation, and variation of precipitation amount affecting Hg wet deposition. Changes in the atmospheric reactants concentrations also increase Hg^0 oxidation and deposition in most regions. The effect of land cover changes on Hg deposition is negligible on a regional scale but can be more noticeable in particular locations, where variation the vegetation coverage is most significant.

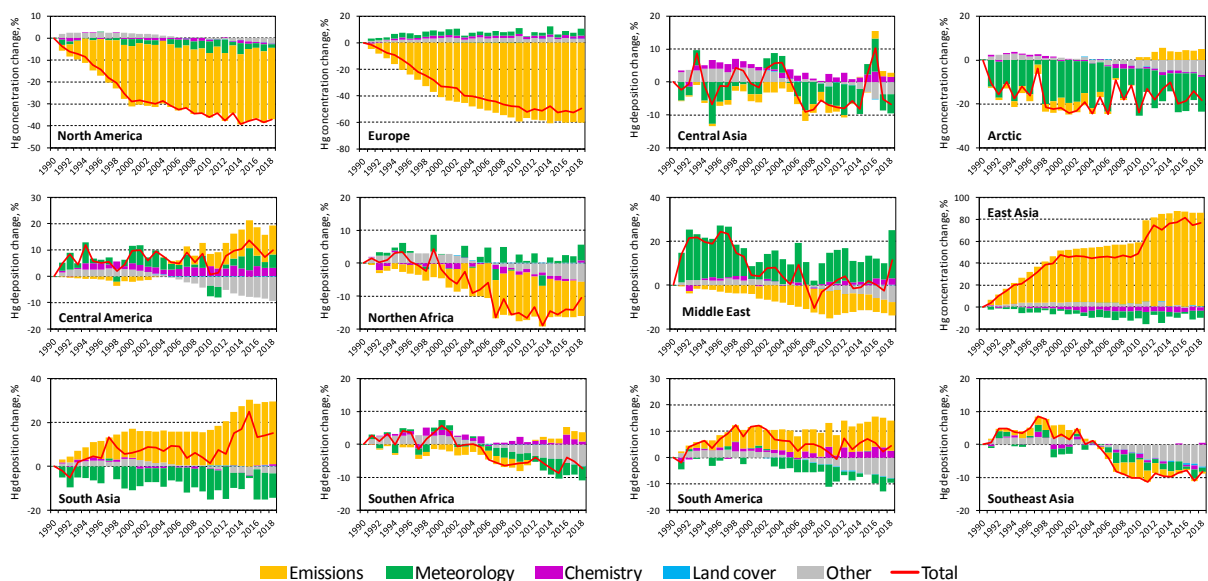


Fig. 19. Contribution of various factors to long-term relative changes of average Hg deposition in various regions. Red line depicts total cumulative change due to all factors.

The presented pilot study illustrates possible approach to analysis and attribution of Hg pollution trends. It should be noted that the performed analysis characterizes just general dependences of the pollution change on variable parameters and does not take into account the effect of changing conditions on particular processes, e.g. Hg^0 air-vegetation exchange, redox atmospheric chemistry, Hg evasion from seawater, soil and snow, etc. More detailed analysis is needed to evaluate the role of physical and chemical processes on temporal dynamics of Hg pollution levels.

3.4. Long-term changes of POP pollution

To illustrate long-term changes of POP pollution, spatial distributions of annual mean modelled concentrations of B(a)P and FLA are presented for 4 selected years (1990, 2000, 2010 and 2018) in Figs. 20 and 21, respectively. Air concentrations in this analysis were calculated as a sum of gas and particle components. The highest B(a)P concentrations are simulated for East Asia followed by South and Southeast Asia as well as the European region. In addition, noticeable concentrations are seen in Central Africa and at the east coasts of North America. This tendency persists throughout all shown years and can be explained by the fact that the concentrations of B(a)P are highly dependent on anthropogenic emissions, which change slowly over a long period. However, B(a)P pollution levels were gradually decreasing from 1990 to 2018 in all regions, except Africa, where pollution remained unchanged, and South Asia, where B(a)P levels slightly increased. The most significant decreases are noticeable in Europe, the southwestern part of Russia and North America.

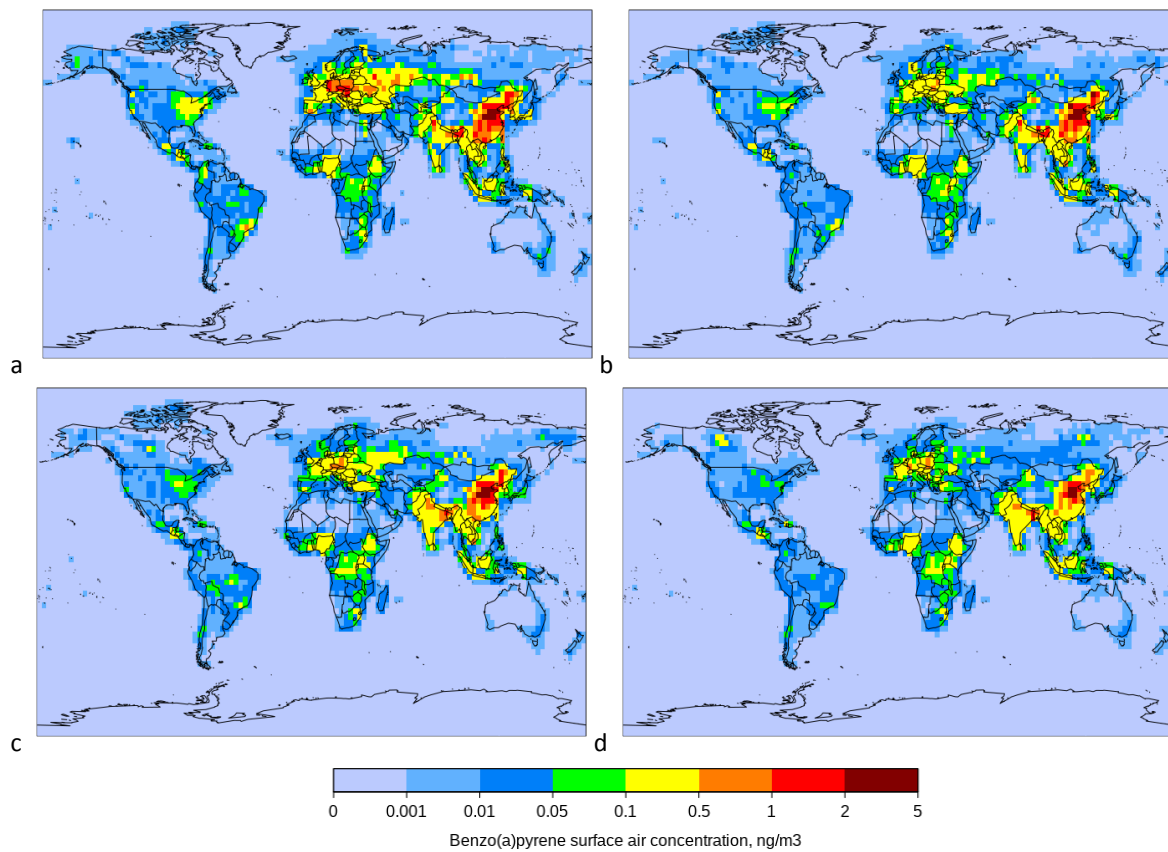


Fig. 20. Global distributions of B(a)P air concentration in 1990 (a), 2000 (b), 2010 (c), 2018 (d).

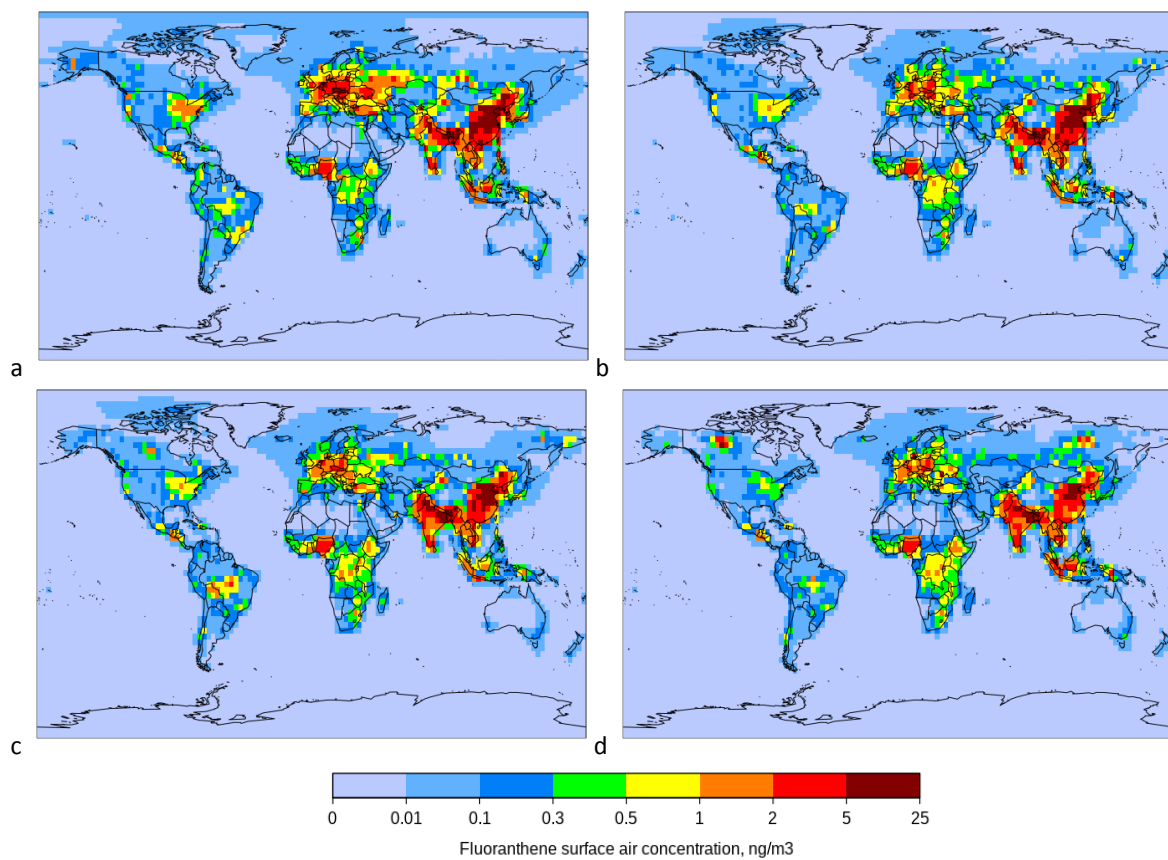


Fig. 21. Global distributions of FLA air concentration in 1990 (a), 2000 (b), 2010 (c), 2018 (d).

The modelled FLA levels are generally much higher compared to B(a)P. Elevated FLA concentrations were predicted for regions with high anthropogenic emissions, namely the European region, both North and South America and Southern Africa. The highest values are noted in South, Southeast and East Asia. The maximum concentrations in these regions are unchanged over all considered years. There is a visible FLA concentration increase between 1990 and 2018 in South Asia and South Africa. In contrast, the concentration decreased in Central and Eastern Europe, in the eastern part of North America and in the middle of South America.

Altogether, model predictions show a tendency towards reduction B(a)P levels in the atmosphere in most parts of the globe. In case of FLA the reduction is not as obvious as in case of B(a)P, but also visible. On the contrary, there are several regions where FLA concentrations in the atmosphere increased. Air concentrations are influenced by various properties of these POPs as well as anthropogenic emissions and meteorological conditions.

3.4.1. Observed and modelled temporal trends

The modeling results for B(a)P and FLA were evaluated against measurement data from the EMEP monitoring network. The available data are limited in terms of temporal coverage. The majority of measurements relate to the last half of the period. Nevertheless, these data can be used for evaluation of both general values and temporal variation of simulated POPs. In particular, long-term data covering more than 10 years of the period are available from 5 and 4 EMEP sites measuring B(a)P and FLA, respectively. The evaluation of the modeling results was performed on a monthly basis to take into account seasonal variation of B(a)P and FLA air concentrations.

Comparison of observed and modelled monthly mean B(a)P and FLA concentrations at selected monitoring sites is illustrated in Fig. 22. The modelling results of B(a)P agree with observations within a factor of two for most monthly values. However, despite good agreement in the summer months, the model tends to underestimate the concentration levels in the winter at some sites, particularly, in Germany, Poland and Finland. At the same time, the model demonstrates good agreement with observations and reproduces the seasonal variation at the sites in Sweden, Slovenia, Latvia, Netherlands and the UK. The model predicts a gradual decrease of the difference between the winter and summer B(a)P levels from 1990 to the end of the period.

There are no significant changes in seasonal variation between modelled summer and winter FLA concentrations, but there is a noticeable decrease in the average annual concentration from 1990 to 2000. In the case of FLA acceptable agreement with measurements is also visible. However, the model underestimates the observed levels at the German and Swedish sites in some winter months.

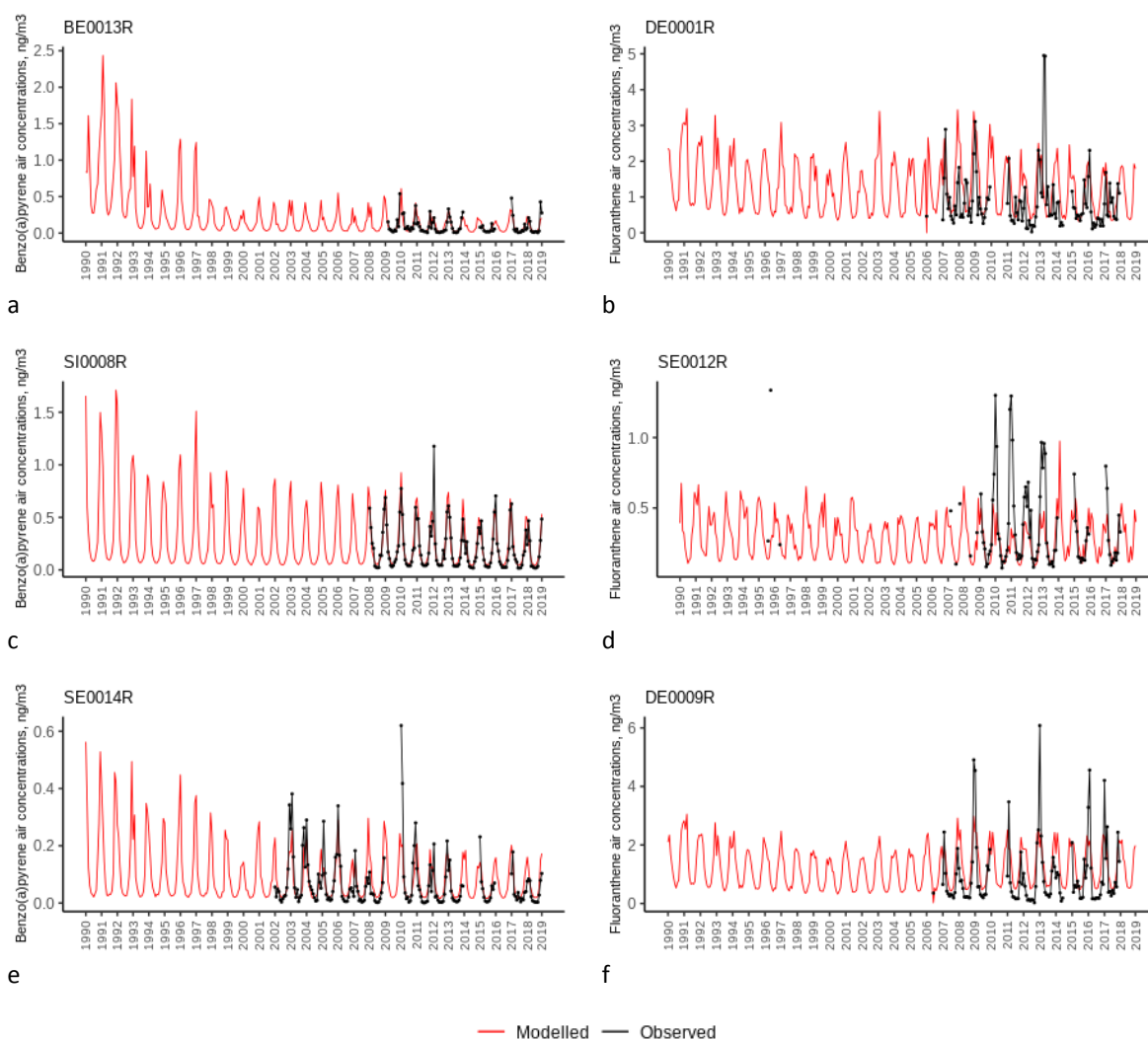


Fig. 22. Comparison of monthly mean modelled and observed air concentrations of B(a)P (a, c, e) and FLA (b, d, f) from 1990 to 2018 at the EMEP measurement sites.

3.4.2. Trends attribution to regional and extra-regional emissions

The source-receptor calculations were carried out for individual years on a global scale. The contribution of regional and extra-regional emission sources to surface air concentrations of B(a)P and FLA in some global regions is presented in Figs. 23 and 24, respectively, for selected years (1990, 1995, 2000, 2005, 2010 and 2015). It should be noted that the source apportionment of B(a)P and FLA air pollution below considers contributions of contemporary anthropogenic emissions only.

According to the modelling results, reduction of both B(a)P and FLA pollution levels caused by anthropogenic emissions is well noticeable in more than half of the regions. The largest B(a)P concentration reductions over 25 years are seen in the Arctic (80%), Europe (70%), Central Asia (66%) and North America (55%). In the case of FLA, the regions that showed the largest decline are Central

Asia (62%), the Arctic (59%), and Europe (47%). Increase of FLA air levels in 2015 compared with 1990 is noted in South Asia (32%) and both parts of Africa (27%). B(a)P levels slightly increased only in Southern Africa (7%).

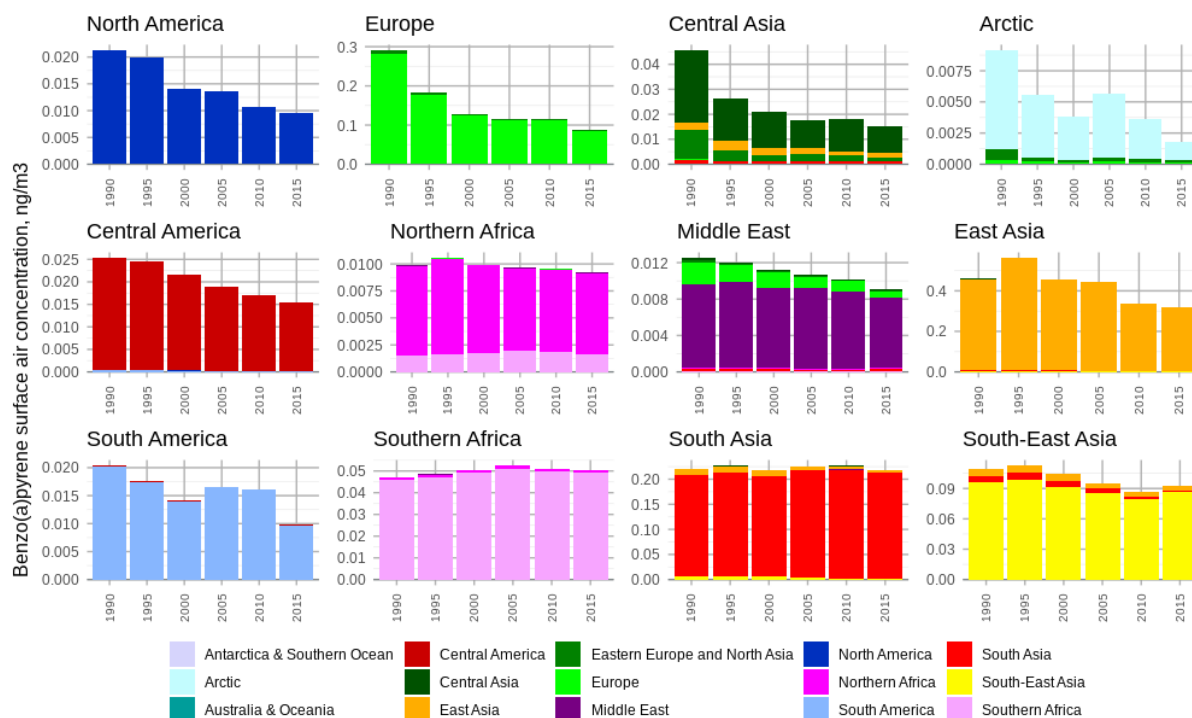


Fig. 23. Source appointment of B(a)P annual mean air concentration from contemporary anthropogenic sources in various regions.

The model assessment of long-range transport shows that intercontinental transport is insignificant for considered PAHs, and regional pollution is mainly caused by the domestic sources. Significant effects from long-range transport can be seen only in regions with low domestic emissions located next to other regions with large emissions. In the case of B(a)P, this takes place for Central Asia, the Middle East, Northern Africa and the Arctic. It can be seen that South and East Asia contribute to B(a)P air pollution of Central Asia and Europe; South Asia contributes to pollution of the Middle East; and Southern Africa contributes to pollution of Northern Africa. Considerable contribution of external sources is noticeable in Europe, Arctic and South Asia. A similar share of contribution of internal and external anthropogenic sources to air concentration in particular regions is a characteristic of FLA. However, the contribution of external sources to air concentration in remote regions for FLA (e.g. the Arctic) is larger than that for B(a)P. Relatively short-range atmospheric dispersion of considered PAHs is caused by their short residence time in the atmosphere with respect to chemical degradation and deposition to the ground.

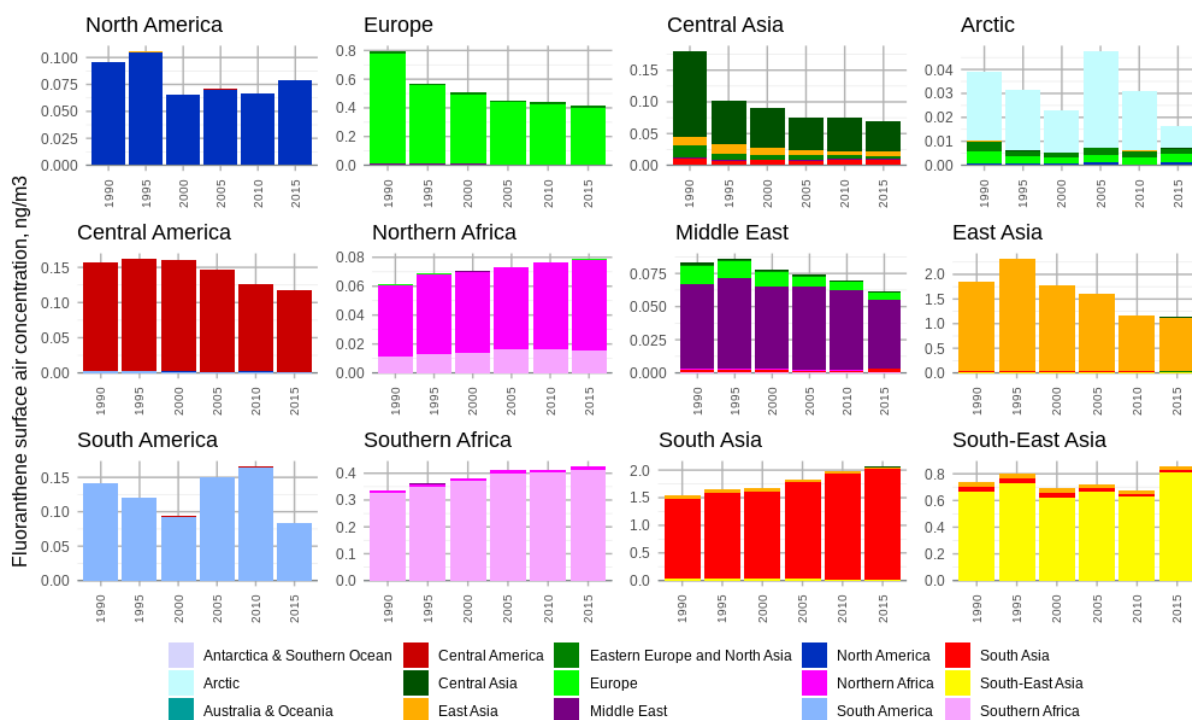


Fig. 24. Source appointment of FLA annual mean air concentration from contemporary anthropogenic sources in various regions.

3.4.3. Trends attribution to environmental factors

The trend attribution analysis allows revealing the influence of changes in emissions and other factors on long-term dynamics of pollution levels. Description of the calculation methods used in the analysis can be found in Section 3.1 of the report. As seen in Figs. 25 and 26, temporal changes of short-lived POPs, such as B(a)P and FLA, are largely determined by variation of anthropogenic emissions. In Europe, North America, Central Asia and the Arctic, where emission was continuously decreasing during the considered period, there is also a considerable decrease in B(a)P and FLA concentration due to this factor. In contrast, in South Asia, where the emission levels of B(a)P are consistently high but show no strong variation throughout the period, changes of air concentrations are small. The increase of FLA levels in both parts of Africa and South Asia is also attributed to increased emissions in these regions. The peaks in relative changes of modelled FLA concentrations in Central America in 1998, in South America in the mid-2010s as well as of both PAHs in Southeast Asia in 1996 are caused by sharp peaks of anthropogenic emissions in these years. Therefore, the results of the analysis are highly sensitive to estimates of temporal changes of emissions and other input parameters.

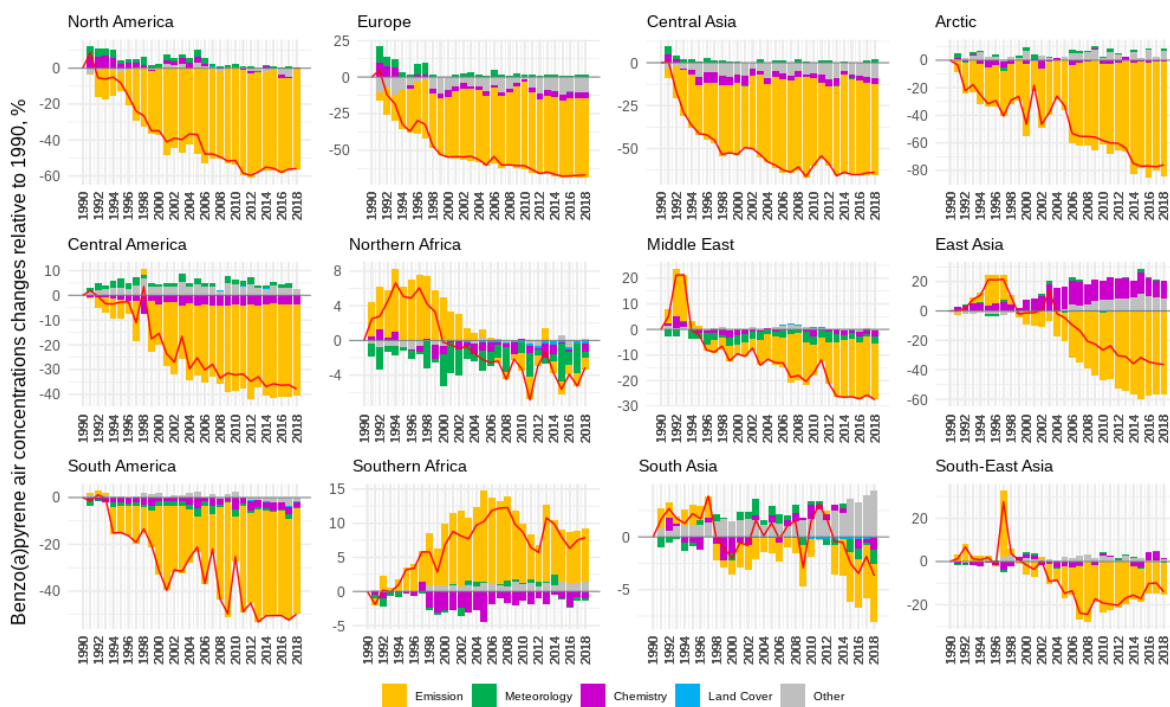


Fig. 25. Contribution of various factors to long-term relative changes of average B(a)P air concentration in various regions. Red line depicts total cumulative change due to all factors.

Other factors also contribute to temporal variability of the concentrations. For instance, short-term increases of both B(a)P and FLA concentrations in 1991 and 1996 in Europe as well as in 1991 and 1994 in North America are mostly caused by meteorological conditions. The strongest effect of meteorological conditions was over Northern Africa for B(a)P and in the Arctic region for FLA. Change in atmospheric chemistry does not significantly affect concentrations of considered substances leading to some additional increase or decrease in particular years. Also, the model simulations show negligible impact of changes in land cover on the PAHs surface air concentrations. This impact is relatively small and ranges from about -0.5 to 0.5% in relative terms. It should be noted that land cover distribution mainly affects dry deposition fluxes rather than atmospheric concentrations. Besides, taking into account significant uncertainties of the land cover data it can be assumed that the use of other datasets can lead to different effects of this factor. Finally, all considered factors do not explain full temporal variability of modelled concentrations. Additional factors are to be identified and evaluated in future.

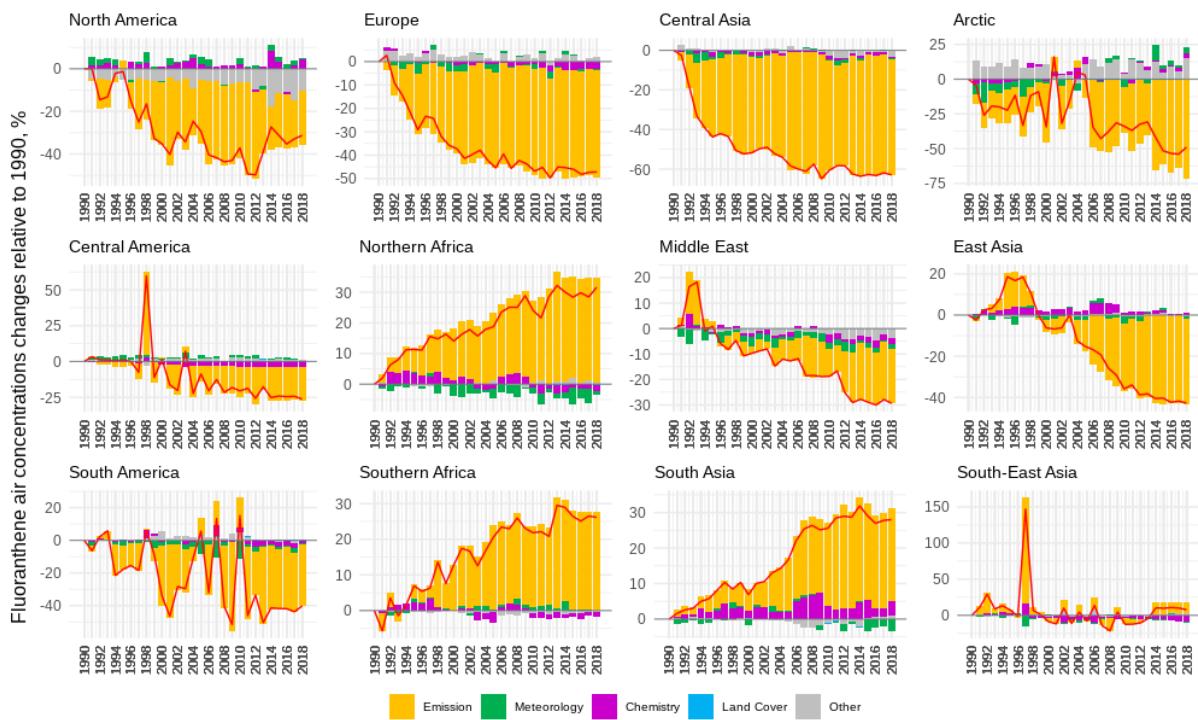


Fig. 26. Contribution of various factors to long-term relative changes of average FLA air concentration in various regions. Red line depicts total cumulative change due to all factors.

4. Concluding remarks

The current progress report contains information on recent activities on Hg and POPs performed in relation to the work under TF HTAP. In particular, in accordance with the bi-annual workplan the Task Force jointly with MSC-E held the workshops that identified current needs in cooperative work to improve Hg and POP pollution assessment and formulated short-term and longer-term plans for future activities.

Attribution of long-term pollution trends is considered as one of the perspective directions of the Task Force future work. To facilitate further discussion and reveal possible issues and uncertainties of the research MSC-E performed pilot simulations and the trend attribution analysis on a global scale. The outcome of the pilot study shows that proposed approach can be applicable and useful for understanding of long-term pollution dynamics. Preliminary results show that long-term changes of the considered pollutants in industrial regions of the globe are largely affected by changes of both regional and extra-regional anthropogenic emissions. The proportion of these contributors varies among the regions and the pollutants of interest. Temporal trends of relatively short-lived PAHs are mostly determined by variation of domestic emissions, whereas changes of long-lived Hg levels undergo considerable effect of intercontinental transport. In addition, the Hg pollution trends are also affected by changes of secondary emissions of legacy Hg accumulated in the environment. Temporal variation of Hg and PAH pollution levels in remote regions are also determined by various environmental factors including meteorological conditions and chemical composition of the atmosphere.

It was concluded that results of the analysis are sensitive to uncertainties of input data on long-term changes of the key parameters affecting levels and variability of the considered pollutants. Estimates of historical and future trends of Hg and POP pollution require reliable data on global anthropogenic and secondary/natural emissions and their changes. Besides, robust information on changes of meteorological conditions, including climate change, altering land cover, sea ice extent, etc., is also needed. In addition, the performed analysis characterizes general dependences of the pollution change on variable parameters and does not consider the effect of changing conditions on the environmental processes (e.g. air-surface exchange, atmospheric chemistry, re-emission from seawater, soil and snow). More detailed analysis is needed to evaluate the role of physical and chemical processes on temporal dynamics of Hg and POP pollution levels.

The future activities on Hg and POPs under TF HTAP in the near-term perspective will include:

- Development and update of global emissions inventories and future scenarios for Hg and POPs and incorporation them into the HTAPv3 global emissions mosaic;
- multi-model study of Hg dispersion and cycling on a global scale with focus on air-surface exchange and secondary/natural emissions;
- global/regional multi-model evaluation of source-receptor relationships for combustion-related POPs (PAHs, PCDD/Fs) in co-operation with the ongoing effort under the EuroDelta-Carb project.

Finally, a communication forum will be established to maintain collaboration across the Hg and POPs scientific communities based on dedicated list servers, quarterly webinars, and data sharing sites as possible mechanisms.

References

- Adler R.F., G.J. Huffman, A. Chang, R. Ferraro, P. Xie, J. Janowiak, B. Rudolf, U. Schneider, S. Curtis, D. Bolvin, A. Gruber, J. Susskind, and P. Arkin [2003] The Version 2 Global Precipitation Climatology Project (GPCP) Monthly Precipitation Analysis (1979–Present). *J. Hydrometeor.*, 4,1147–1167.
- AMAP/UNEP [2013] Technical Background Report for the Global Mercury Assessment 2013. Arctic Monitoring and Assessment Programme, Oslo, Norway/UNEP Chemicals Branch, Geneva, Switzerland. vi + 263 pp.
- AMAP/UNEP [2019] Technical Background Report for the Global Mercury Assessment 2018. Arctic Monitoring and Assessment Programme, Oslo, Norway/UN Environment Programme, Chemicals and Health Branch, Geneva, Switzerland. viii + 426 pp including E-Annexes.
- Colette A. et al. [2016] Air pollution trends in the EMEP region between 1990 and 2012. EMEP: CCC-Report 1/2016, Kjeller, Norway.
- ECMWF [2021] Operational archive. <https://www.ecmwf.int/en/forecasts/dataset/operational-archive>. Last access: 14 July 2021.
- Ferrari C.P., Padova C., Faïn X., Gauchard P.-A., Dommergue A., Aspino K., Berg T., Cairns W., Barbante C., Cescon P., Kaleschke L., Richter A., Wittrock F., Boutron C. (2008) Atmospheric mercury depletion event study in Ny-Alesund (Svalbard) in spring 2005. Deposition and transformation of Hg in surface snow during springtime. *Sci. Total Environ.* 397, 167–177.
- Friedl M., Sulla-Menashe D. [2019] *MCD12Q1 MODIS/Terra+Aqua Land Cover Type Yearly L3 Global 500m SIN Grid V006* [Data set]. NASA EOSDIS Land Processes DAAC. Accessed 2021-05-14 from <https://doi.org/10.5067/MODIS/MCD12Q1.006>.
- HTAP [2010a] Hemispheric transport of air pollution 2010. Part B: Mercury. Air pollution studies No. 18. Pirrone N. and Keating T. (Eds.) UN Economic Commission for Europe, Geneva. pp. 211. doi: [10.18356/1415ffe5-en](https://doi.org/10.18356/1415ffe5-en).
- HTAP [2010b] Hemispheric transport of air pollution 2010. Part C: Persistent Organic Pollutants. Air pollution studies No. 19. Dutchak S. and Zuber A. (Eds.) UN Economic Commission for Europe, Geneva. pp. 257. doi: [10.18356/b73bba7e-en](https://doi.org/10.18356/b73bba7e-en).
- Ilyin I., N.Batrakova, A.Gusev, M.Kleimenov, O.Rozovskaya, V.Shatalov, I.Strijkina, O.Travnikov, K.Breivik, H.L.Halvorsen, P.B.Nizzetto, K.A.Pfaffuffer, W.Aas, K.Mareckova, S.Poupa, R.Wankmueller, B.Ullrich [2021] Heavy metals and POPs: Pollution assessment of toxic substances on regional and global scales. EMEP Status Report 2/2021.
- Johnson K.P., Blum J.D., Keeler G.J., Douglas T.A. (2008) Investigation of the deposition and emission of mercury in arctic snow during an atmospheric mercury depletion event. *J. Geophys. Res. Atmos.* 113, D17304.
- Kirk J.L., St Louis V.L., Sharp M.J. (2006) Rapid reduction and reemission of mercury deposited into snowpacks during atmospheric mercury depletion events at Churchill, Manitoba, Canada. *Environ. Sci. Technol.* 40, 7590–7596.
- Muntean M., Janssens-Maenhout G., Song S., Giang A., Selin N.E., Zhong H., Zhao Y., Olivier J.G.J., Guizzardi D., Crippa M., Schaaf E., Dentener F. [2018] Evaluating EDGARv4.0tox2 speciated mercury emissions ex-post scenarios and their impacts on modelled global and regional wet deposition patterns. *Atmospheric Environment* 184, 56–68. <https://doi.org/10.1016/j.atmosenv.2018.04.017>.
- Shen H, Huang Y, Wang R, Zhu D, Li W, Shen G, Wang B, Zhang Y, Chen Y, Lu Y, Chen H, Li T, Sun K, Li B, Liu W, Liu J, Tao S. [2013] Global atmospheric emissions of polycyclic aromatic hydrocarbons from 1960 to 2008 and future predictions. *Environ Sci Technol.* 2013 Jun 18;47(12):6415–24. doi: 10.1021/es400857z. Epub 2013 May 31. PMID: 23659377; PMID: PMC3753807.
- Skamarock W.C., Klemp J.B., Dudhia J., Gill D.O., Barker D.M., Duda M.G., Huang X.-Y., Wang W. and Powers J.G. [2008]. A Description of the Advanced Research WRF Version 3. NCAR/TN–475+STRNCAR TECHNICAL NOTE.
- Streets D.G., Horowitz H.M., Lu Z., Levin L., Thackray C.P., Sunderland E.M. [2019a] Five hundred years of anthropogenic mercury: spatial and temporal release profiles. *Environ. Res. Lett.* 14, 084004. doi: 10.1088/1748-9326/ab281f.
- Streets D.G., Horowitz H.M., Lu Z., Levin L., Thackray C.P., Sunderland E.M. [2019b] Global and regional trends in mercury emissions and concentrations, 2010–2015. *Atmospheric Environment* 201, 417–427. doi: 10.1016/j.atmosenv.2018.12.031.
- Travnikov O. and Ilyin I. (2009) The EMEP/MS-CHEM mercury modeling system. In: Mercury Fate and Transport in the Global Atmosphere, R. Mason, N. Pirrone (Eds). Springer, Boston, pp. 571–587.

- Travnikov O., Angot H., Artaxo P., Bencardino M., Bieser J., D'Amore F., Dastoor A., De Simone F., Diéguez M. D. C., Dommergue A., Ebinghaus R., Feng X. B., Gencarelli C. N., Hedgecock I. M., Magand O., Martin L., Matthias V., Mashyanov N., Pirrone N., Ramachandran R., Read K. A., Ryjkov A., Selin N. E., Sena F., Song S., Sprovieri F., Wip D., Wängberg I., and Yang X. [2017] Multi-model study of mercury dispersion in the atmosphere: atmospheric processes and model evaluation, *Atmos. Chem. Phys.*, 17, 5271-5295, doi:10.5194/acp-17-5271-2017.
- Travnikov O., Batrakova N., Gusev A., Ilyin I., Kleimenov M., Rozovskaya O., Shatalov V., Strijkina I., Aas W., Breivik K., Nizzetto P.B., Pfaffhuber K.A., Mareckova K., Poupa S., Wankmueller R., Seussall K. [2020] Assessment of transboundary pollution by toxic substances: Heavy metals and POPs. EMEP Status Report 2/2020.
- UNEP [2017] Global Monitoring Plan for POPs under the Stockholm Convention. UN Environment. Available at <http://chm.pops.int/Portals/0/download.aspx?d=UNEP-POPS-COP.8-INF-38.English.pdf>.